Journal of Lie Theory
Volume **32** (2022) 709–736

Differential Invariant Signatures for Planar Lie Group Transformations with Application to Images

Richard Brown, Stephen Marsland, Robert McLachlan

Communicated by P. J. Olver

Abstract. The actions of various Lie groups underlie the change of appearance of objects in images as the viewpoint changes, e.g., through camera motion. Despite significant advances in object recognition using machine learning in recent years, the question of how to recognise an object in an image as its appearance varies through camera motion and similar effects remains open. We demonstrate how differential invariant signatures can be derived for each of the transformation groups, and how the underlying invariances reflect the group-subgroup structure of the relevant Lie groups.

There are a variety of methods that can be used to identify differential invariants, and we provide examples of three of them: tensor contraction, transvectants, and the method of moving frames. We use the resulting invariants to construct practical sets to form three-dimensional invariant signatures. These signatures are not necessarily complete: the image cannot always be reconstructed uniquely up to transformation, but they are plottable, and depend at worst on third derivatives, although more channels of information, such as colour images, can reduce the highest order of derivative needed in some cases. We demonstrate the invariant signatures for each transformation group based on a simple smooth image. A full consideration of how these signatures could be used in practice will require effective methods to numerically approximate derivatives for images.

Mathematics Subject Classification: 65D18, 53A55, 68U10.

Key Words: Object recognition, planar transformation, planar Lie groups, invariants, differential invariant signature.

1. Introduction

The appearance of a fixed object in a set of images can vary markedly depending upon such variables as pose and position relative to the camera, even though the object itself does not change. This is even more marked in scenes that consist of multiple objects at different distances and orientations to the camera against a fixed background. The appearance of each individual object will then change in different ways as a constant camera motion or other such transformation is applied. The individual transformations will appear as the action of an element of a planar Lie group, for example the affine, or projective groups, or an angle-preserving transformation from the conformal group, depending upon the camera model.

It is therefore natural to seek representations of objects that do not change as these various transformation groups act. If the space of objects is denoted M and the transformations form a Lie group $\mathcal{G}$, then mathematically one seeks a way to study objects in $M/\mathcal{G}$, such as by seeking $\mathcal{G}$-invariant functions on M. Mathematical

ISSN 0949–5932 / $2.50

invariants provide a useful way to identify sets of objects that are the same up to some equivalence relation, since the functions are constant for objects in the same equivalence class (orbits of the group). For images, rather than considering the image of the object, one constructs an invariant signature of some kind, which represents the object modulo the action of elements from the relevant group. This has been considered extensively by Olver and co-authors for the case of outlines of objects [6, 24]. We extend this by considering the case of signatures for images rather than outlines of curves under a variety of planar Lie transformation groups, particularly those of relevance to image analysis.

In this paper our aim is to follow the mathematical underpinnings of constructing differential invariant signatures for images under the action of (nested) planar Lie groups, and to summarise the impediments to a practical implementation, including the number of derivatives required. We demonstrate three distinct methods of computing differential invariants: by tensor contraction, using the theory of transvectants, and via the method of moving frames, applying the methods to a variety of the planar Lie groups, and providing sample signature sets for the various groups we consider, together with an example of a sample signature surface based on a random transformation of a simple, smooth image.

1.1. Invariant signatures of images

A greyscale image can be viewed as a two-dimensional manifold embedded in a three dimensional ambient space, with coordinates $(x, y, f(x, y))$. A signature $\mathcal{I}(f) \in \mathbb{R}^m$ has coordinates $\mathcal{I}(f) = (I_1, I_2, \ldots, I_m)$, where each I_i is a function of $f(x, y))$ and its derivatives, and will therefore be a two-dimensional manifold embedded in $\mathbb{R}^m$. Under a change of coordinates $(x, y) \mapsto (\bar{x}, \bar{y})$ induced by a group action, the signatures of the original image and transformed version $\bar{f}(\bar{x}, \bar{y}) = f(x, y)$ will be the same. The introduction of an invariant signature reduces the object recognition problem modulo some transformation group to one of comparing the signatures of the objects, rather than the images themselves. We do not consider the question of classification further in this paper; a standard image recognition algorithm can be used (see, e.g., [62] for a survey), or a matching method such as [4] can be used.

We define a *k-colour image* as a triple (f, Ω, k) where $\Omega \subset \mathbb{R}^n$ (typically, images are planar, so $n = 2$), $1 \leq k \in \mathbb{Z}$ is the number of colour channels, and $f \colon \Omega \to \mathbb{R}^k$. The function f will be taken to be as smooth as necessary. Consider a (finite or infinite-dimensional) local transformation group $\mathcal{G}$. A transformation $\varphi \in G$ acts on images by $\varphi \cdot (f, \Omega, k) = (f \circ \varphi^{-1}, \varphi(\Omega), k)$. We mostly consider greyscale images, so $k = 1$. Also, since we work locally, we will usually omit the domain Ω.

In order to define differential invariants, it is necessary to identify how the group transformation φ acts on derivatives of the function f via the jet space [31, 41]. The d-th order jet space J^d is coordinatised by the function itself and the set of all partial derivatives of the function up to order d.

(Note that there are $\binom{d+k-1}{k}$ partial derivatives of order d.)

As the group $\mathcal{G}$ is local, it acts naturally on derivatives of the transformation, and so each individual transformation $\varphi \in \mathcal{G}$ can be prolonged to act on the jet space J^d. We can thus prolong the action of the group and consider the action of $\mathcal{G}$ on not just f, but all derivatives of f up to order d. A d-th order differential invariant is then a

local scalar function $I : J^d(f, \Omega, k) \to \mathbb{R}$ that is invariant under the action of $\mathcal{G}$, i.e., $I(\varphi(f, \Omega, k)) = I(f, \Omega, k) \forall \varphi \in \mathcal{G}$. It can also be useful to consider the maximum order of derivative in the invariant, which we term the degree, e.g., $f_{xy}^2 f_x f_y$ has degree 2.

The methods we use to construct the invariants, particularly the moving frame, produce invariants that are singular at points such as critical points. In all groups considered the invariants are rational functions of the derivatives of the function. Moreover, the denominators of these functions are powers of each other, and so it is possible to clear the denominators, thereby removing the singularity, by a projection technique that will be introduced in Section 2.3.

For the case of two-dimensional greyscale images it is often convenient to work in coordinates. In this case the transformation group action by a coordinate transformation $\varphi \colon \mathbb{R}^2 \to \mathbb{R}^2$ is given by (where f and $\mathbf{x}$ denote the original image and coordinates, and $\bar{f}$ and $\bar{\mathbf{x}}$ the transformed versions):

$$\mathbf{x} \mapsto \bar{\mathbf{x}} = \varphi(\mathbf{x}). \tag{1}$$

The transformed image is then defined to be:

$$\bar{f}(\bar{\mathbf{x}}) = (f \circ \varphi^{-1})(\bar{\mathbf{x}}) = f(\mathbf{x}). \tag{2}$$

Derivatives of $\bar{f}$ and f can be related by the chain rule, for example the first order derivatives are given by:

$$f_x = \bar{f}_{\bar{x}} \bar{x}_x + \bar{f}_{\bar{y}} \bar{y}_x \quad \text{and} \quad f_y = \bar{f}_{\bar{x}} \bar{x}_y + \bar{f}_{\bar{y}} \bar{y}_y \tag{3}$$

where $\bar{x}_x = \frac{\partial \varphi_1}{\partial x}(x, y)$, et cetera.

A signature set is the image of m invariants $\mathcal{I} = (I_1, I_2, \ldots, I_m)$. For simplicity of notation we will write $\mathcal{I}(f) \subset \mathbb{R}^m$ with the understanding that each signature component is actually acting on the jet space $J^d(f, \Omega, k)$; see Section 2.1 for a basic example. A signature set is complete for f if it determines f up to transformations from $\mathcal{G}$, i.e., if $\mathcal{I}(\tilde{f})(\tilde{\Omega}) = \mathcal{I}(f)(\Omega)$ implies that there exists a transformation $\varphi \in \mathcal{G}$ such that $\tilde{f} = \varphi \cdot f$ and $\tilde{\Omega} = \varphi(\Omega)$.

Ideally, an invariant signature would be complete, so that the image is exactly determined by the signature up to a transformation, and two objects share a signature if and only if they differ only by a transformation from $\mathcal{G}$. However, there are some pathological scenarios that occur regularly in images, particularly that flat regions of images collapse down to single points in the signature (as all of the derivatives are zero in these regions). Then images that are otherwise similar (apart from the size of one of these regions) cannot be distinguished. However, the number of dimensions m of the ambient manifold can increase markedly for complete signatures, increasing the computational cost and making it impossible to visualise the signature surface. For many applications an incomplete signature is sufficient, and is what we consider here, favouring signatures in three coordinates, since for greyscale images, $\mathbb{R}^3$ is the smallest space in which the signature surfaces can reside. If the signature is not complete, then there will be a 'bad set' of images that cannot be distinguished from each other. The codimension of the bad set is defined as the difference between the dimensionalities of the whole space and of the bad set. The codimension should ideally be large, meaning that the dimension of the bad set would be small.

In addition to a bad set of high codimension, in order for the invariant signatures to be useful to identify similarity in images, there are two other key considerations: they must vary continuously with respect to the image, and they must be robust with respect to occlusions, where one object obscures some part of another. These constraints are essential if the signature is to be used to detect similarity of images, but the first fails for the rational invariants found in the literature. Such considerations lead one naturally to consider local invariants, i.e., those defined using each point of the object as its own basepoint, together with a neighbourhood in some topology. This is sufficient to compute, e.g., derivatives of an object. For this reason we focus on differential invariants. The disadvantage of such invariants, as we shall discuss, is the need to compute several orders of spatial derivative of the image. See [38] and references therein for more discussion about the desirable properties of a set of invariants for image and curve analysis.

1.2. Relevant groups

The set of groups that we consider are shown as a lattice in Figure 1, where the size of the groups decrease down the page, and the arrows denote the subgroup relationship. There is an important relationship between a group and its subgroups for invariants, which is that invariants of a group are automatically invariants of its subgroups. This means that care is needed to distinguish between the two, with further invariants that are known not to be invariant in the supergroup included. The finite-dimensional groups in this lattice were chosen because they are the only planar Lie groups that include translation and have locally primitive algebras (that is, for any open subset of the plane, there is no one-dimensional foliation that is left invariant by the action of the corresponding group [20]). This makes them the groups most directly relevant to image transformations. The infinite-dimensional (pseudo-Lie) examples are likewise those most likely to be of interest for image transformation, in particular the full diffeomorphism group, which is commonly used for image registration for medical images, see e.g., [61].

1.3. Relevant literature

The theory of invariants has a rich mathematical history, starting from invariants of forms [9], where the invariants are polynomials in the coefficients of the forms, see e.g., [30, 42] for an overview. Geometric considerations and differential invariants followed fairly quickly [5, 48, 54, 59], particularly because they enabled the classification of differential equations into equivalence classes [8, 34, 35]. More recently, this has been extended, primarily by Olver and collaborators, see e.g., [41] and [42] for summaries.

There has been a long-standing interest in constructing invariants for image recognition and pattern analysis, see e.g., [39] and [60]. This was set in the context of Lie's invariants by [58], where the concept of a joint (or semi-) differential invariant (an invariant that acts on the joint action of the transformation group, see [12, 43]) was introduced [57]; see also [26].

A variety of function spaces have allowed for the creation of different sets of invariants for particular groups. For the Euclidean group, the Fourier transform provides a useful tool [18, 19, 51, 56], and this can be extended to the affine group using the Fourier-Mellin transform [49, 63] and the bispectrum [28, 40]. Alternatively, integral

invariants [15, 36] and geometric moments can be computed. For the similarity group applied to images the original reference is [25], but see also [23] for affine transformations, [17] for an implicit representation, and [47] for their use in a binary pattern for image recognition, which is somewhat related to the invariant features such as SURF [3].

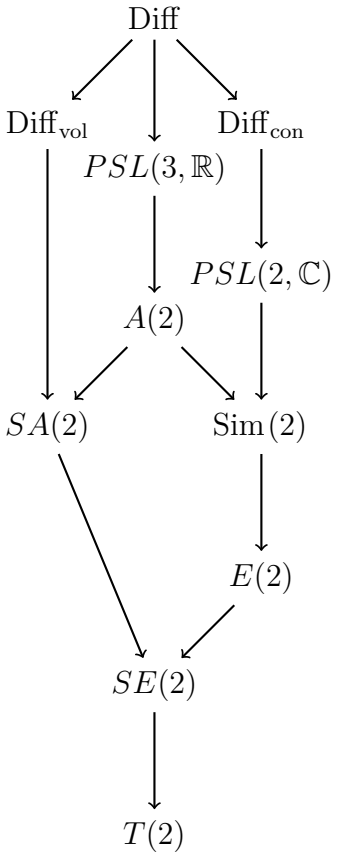

Figure 1: The lattice of groups considered in this paper. The edges identify subgroups.

The group that has been of particular interest for image analysis is the projective group, because of its ubiquity in camera models. Invariants for this group have been computed using points [21, 52], geometric moments [53], curvature [22], and differential and joint invariants [2, 27, 29, 33]. In particular Olver, in [46], uses the same approach as we do in §4.4, but with a different moving frame normalization to produce a different set of projective image invariants.

Although there are computational challenges regarding the numerical approximation of derivatives on images, the fact that differential invariants are robust to occlusion, cheap to compute, and are based on local computations, has made them popular for researchers in image analysis [16]. Two particular tools have been key to this: Cartan's moving frame [7] (see Section 4), which was used to construct image invariants as early as 1994 by [11], and the concept of an image signature built from a set of invariants [6]. An algorithm to compute differential and joint invariants and determine complete signature sets is described by [44, 45] The entire set of invariants is computed using the method of moving frames and then the signature set of a maximal set of functionally independent invariants is identified. A third step

is possible, in which the dimension of the signature set is reduced by eliminating those invariants whose values can be computed from the values of derivatives of some subset of the invariants. Further work, including applications to ODEs and the Calculus of Variations can be found in [37].

2. Differential invariants by direct computation

2.1. Translations

The most basic transformation group of a image is the translation group $T(2)\colon \mathbb{R}^2 \to \mathbb{R}^2$ with elements of the form $\varphi(\mathbf{x}) = \mathbf{x}+\mathbf{t}$ for fixed $\mathbf{t}$. These could arise from actions such as cropping a photo.

We could explicitly write the calculation in Eq. 3 for this case, but instead provide an intuitive explanation. Consider a point in the original image, and the corresponding point in the transformed one. Clearly, the intensity value of the points match, and so do their first spatial derivatives. These three quantities can be used as coordinates in a new space, where the two image points will correspond. Computing these coordinates for all image points will define a surface in the new three-dimensional space, and the two images will produce the same surface, the signature, $\mathcal{I}(f)(x,y) = (I_1, I_2, I_3)$ where $I_1 = f, I_2 = f_x, I_3 = f_y$.

For each signature set that we derive, it is informative to see an example signature of the kind of surface that is defined, normally a two-dimensional surface in three-dimensions. We will apply a small random transformation from the relevant group to a single continuous image and plot the signature before and after this transformation has been applied. This is an aid to understanding rather than any form of demonstration of the robustness of our signature sets.

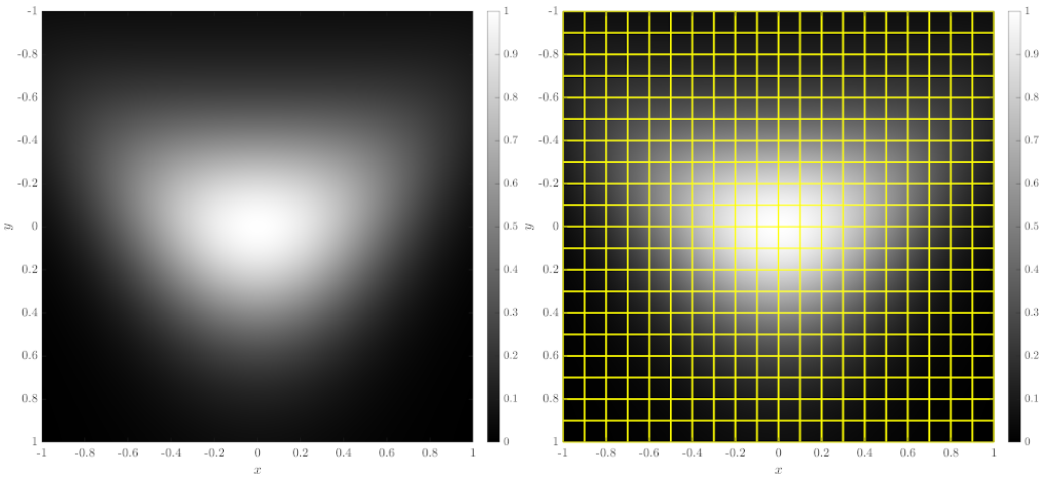

Figure 2: The test function used as an image, defined in Eq. (4). On the left the image itself is shown, while on the right a version with a regular grid superimposed is given.

The image we use is a continuous function (thus avoiding numerical issues in the approximation of derivatives) defined on $[-1,1] \times [-1,1]$ as:

$$f(x,y) = \exp(-2x^2 - 4\sin^2(y + 0.5x^2)) \tag{4}$$

The function is depicted as a greyscale image in Fig. 2. We will use this function throughout, using the grid on the right of the figure to help visualise both the transformation and how the image is mapped into the three-dimensional signature surface. Note that there is nothing particularly special about this particular function; it has relatively well-behaved derivatives, includes a critical point, and decays towards the boundary of the image.

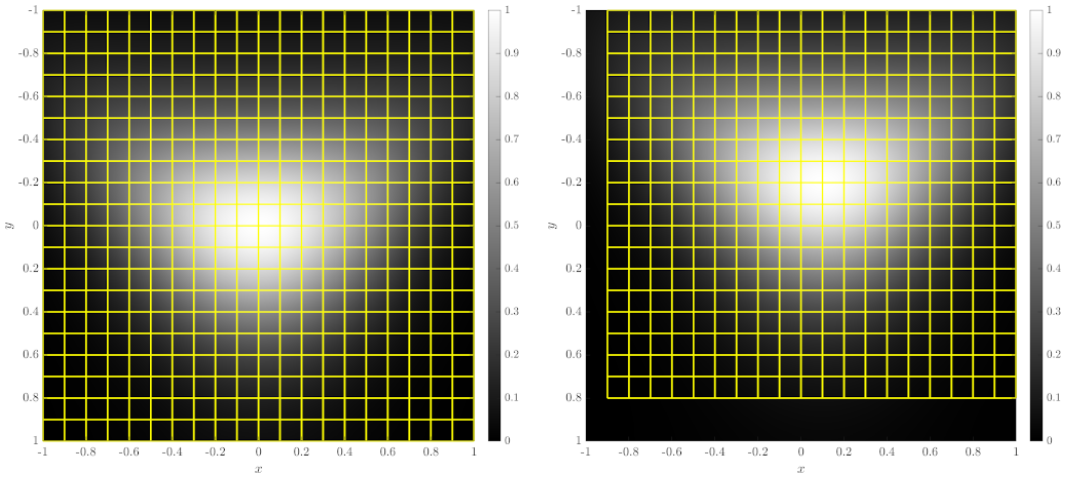

(a) (b)

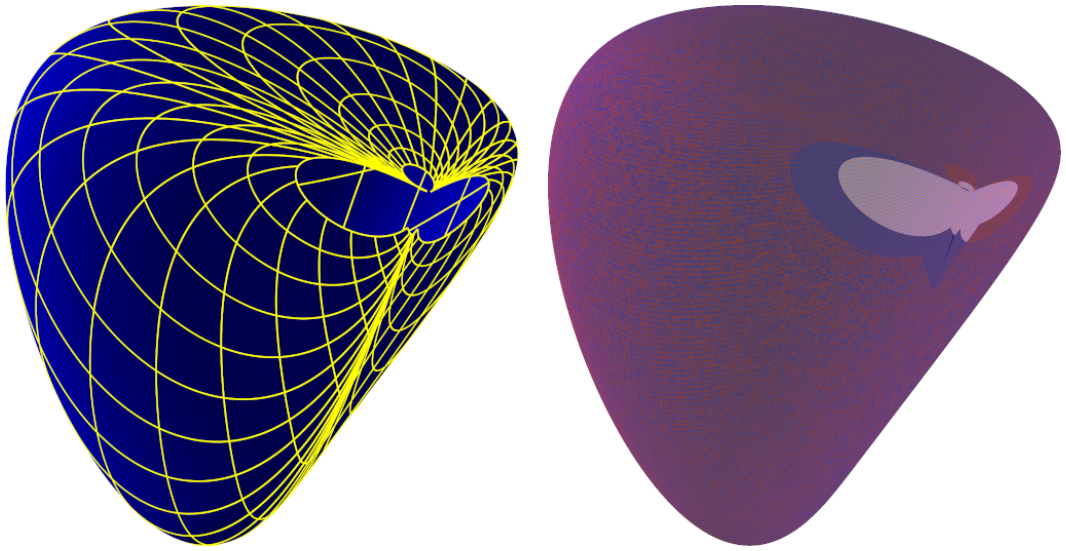

(c) (d)

Figure 3: (a), (b) The image before and after the $T(2)$ transformation $(x, y) \mapsto (x + 0.1, y - 0.2)$. (c) the signature of the image (before translation). (d) the signatures before (blue) and after (red) the translation superimposed, showing that the signature surface is invariant.

Fig. 3 shows (a) the original image, (b) the translated image under the transformation $(x, y) \mapsto (x+0.1, y-0.2)$, (c) the signature of one of them, (d) the superimposed pair of signatures. The yellow lines in (c) correspond to places where the yellow grid from (a) has been mapped to on the signature surface. The parts of the surface where the mesh gets close together are where the function and its derivatives are tending towards zero. This occurs around the boundary of our test image and so

all of these points are close together in the signature space. In (d), notice that as some of the image has moved out of frame, there are parts of the signature surfaces of the two images that do not overlap.

2.2. Differential invariants through tensor contraction

While we avoid the use of tensors in most of this study, there is a notable exception to be made for the Euclidean transformation group $E(2)$. In this setting we can restrict ourselves to *Cartesian tensors*, where we need make no distinction between covariance and contravariance as they are equivalent. We therefore use subscript indices exclusively.

In this setting, a Euclidean transformation acting on $\mathbb{R}^2$ is given by an expression of the form:

$$\bar{x}_i = a_{ij}x_j + b_j,$$

using the Einstein summation convention. The orthogonality condition is that $a_{ik}a_{jk} = a_{ki}a_{kj} = \delta_{ij}$. A Euclidean transformation $\varphi\colon \mathbb{R}^2 \to \mathbb{R}^2$ can also be written in matrix form as $\bar{\mathbf{x}} = \varphi(\mathbf{x}) = U\mathbf{x} + \mathbf{t}$ where the matrix U satisfies $U^TU = I$ and $\mathbf{t} \in \mathbb{R}^2$.

With respect to $\mathbb{R}^2$, a Cartesian tensor of rank p, or p-tensor is a 2^p-tuple of real numbers $C_{i_1\ldots i_p}$ whose components transform under a Euclidean transformation as:

$$\bar{C}_{i_1\ldots i_p} = a_{i_1j_1}\cdots a_{i_pj_p}C_{j_1\ldots j_p}$$

and a 0-tensor is a scalar, or invariant.

The main observation is that in this setting, the n^{th} order partial derivative operator $\partial^n/\partial_{x_{i_1}}\cdots\partial_{x_{i_n}}$ formally transforms as an n-tensor, [16]. Because the product of a p-tensor and a q-tensor gives a $(p+q)$-tensor and contraction of a p-tensor yields a $(p-2)$-tensor, a complete contraction of a tensor of even rank formed as a product of terms of the form $\partial^p f/\partial_{x_{i_1}}\cdots\partial_{x_{i_p}}$ will give a Euclidean invariant.

For example, up to second derivatives, we have the following Euclidean invariants, expressed as tensor contractions:

$$\begin{aligned} I_0 &= f = f\,, \\ I_1 &= f_i f_i = f_x^2 + f_y^2\,, \\ I_2 &= f_{ii} = f_{xx} + f_{yy}\,, \\ I_3 &= f_{ij}f_{ij} = f_{xx}^2 + 2f_{xy}^2 + f_{yy}^2\,, \\ I_4 &= f_i f_j f_{ij} = f_x^2 f_{xx} + 2f_x f_y f_{xy} + f_y^2 f_{yy}\,. \end{aligned} \tag{5}$$

While we can construct any number of invariants this way, there is no guarantee of functional independence between them. We will address this issue in Section 4 when we construct invariants of $E(2)$ and other groups using the method of moving frames. We can form a signature from any three of the invariants in Eq. (5), for simplicity we choose our signature to be:

$$\mathcal{I}_{E(2)} = (I_0, I_1, I_2). \tag{6}$$

A sample $E(2)$ transformation is depicted in Fig. 4 with its corresponding signature.

We will defer discussion of the Special Euclidean group (which excludes reflections) until Section 4.1, where suitable invariants naturally arise from the method of moving frames.

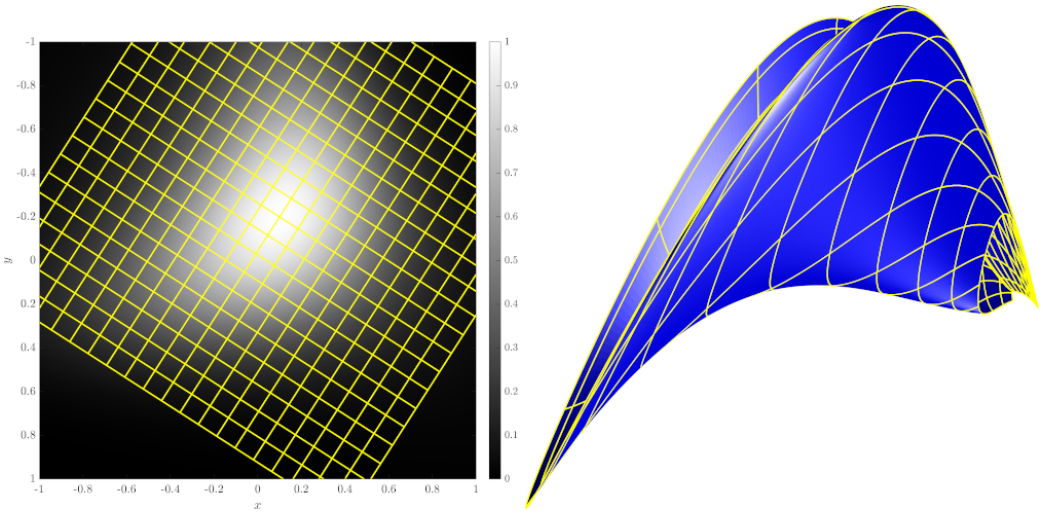

Figure 4: A sample $E(2)$ Transform and 3D signature.

2.3. The similarity group

The similarity group $\mathrm{Sim}(2)$ consists of transformations of the form $\bar{\mathbf{x}} = \varphi(\mathbf{x}) = sU\mathbf{x} + \mathbf{t}$, where $U^T U = I$ and $s \in \mathbb{R} \setminus \{0\}$. It is like the Euclidean group except it also allows for isotropic scaling. In image applications, similarity transformations arise from operations like zooming.

Under transformations by $\mathrm{Sim}(2)$, the Euclidean invariants become *relative* invariants, i.e., each derivative introduces a multiple of s to each invariant. For example, $\bar{f}_{\bar{x}}^2 + \bar{f}_{\bar{y}}^2 = s^2(f_x^2 + f_y^2)$ and $\bar{f}_{\bar{x}\bar{x}}^2 + 2\bar{f}_{\bar{x}\bar{y}}^2 + \bar{f}_{\bar{y}\bar{y}} = s^4(f_{xx}^2 + 2f_{xy}^2 + f_{yy}^2)$. We refer to the power of s as the weight of the transformation. The concept of a relative invariant will be important in the rest of this paper. It follows the definition given here, except that the function weighting the invariant is more general, see [12] for more details. In contrast to that paper, we will continue to use the term weight to represent the power to which the function is raised.

One way to produce similarity invariants would be to take ratios of powers of the Euclidean invariants (5) so that the multiples of s cancel. For example $\frac{f_x^2+f_y^2}{f_{xx}+f_{yy}}$ is the ratio of two weight-2 relative invariants and is hence a similarity invariant. However, this invariant is singular whenever $f_{xx} + f_{yy} = 0$, which is a codimension 0 phenomenon for images.

A better approach is to take three invariants of the same weight. Taking I_1^2, I_2^2, and I_3 from (5), all of which are weight 4, defines a surface up to scale, and so they can be projected on to the unit sphere. We therefore multiply by another invariant to form the signature surface; an appropriate choice is $I_0 = f$. This signature is defined by:

$$\mathcal{I}_{\mathrm{Sim}(2)}(f) = \frac{f}{\sqrt{I_1^4 + I_2^4 + I_3^2}}(I_1^2, I_2^2, I_3). \tag{7}$$

It is only singular when $f_x = f_y = f_{xx} = f_{yy} = f_{xy} = 0$. A sample similarity transformation and computed signature is shown in Fig. 5.

3. Differential invariants through transvectants

Another way to compute invariants is to compare the simultaneous action of a group element on separate copies of the underlying space (for planar images, $\mathbb{R}^2$).

By identifying these spaces with each other it is possible to construct a function known as a transvectant that is a relative invariant to that group action.

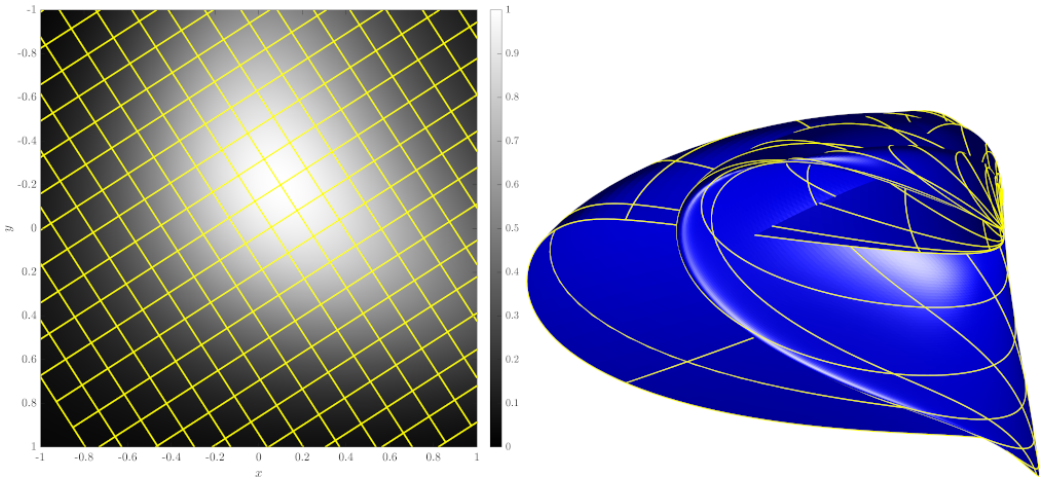

Figure 5: A sample Sim(2) transform and 3D signature.

We will demonstrate this for the affine group $A(2)$ and its subgroup $SA(2)$ where, following the treatment by [42], this leads to Cayley's Omega Process [10].

Consider $\mathbf{x}_i \in \mathbb{R}^2, i = 1, 2$, so that $\mathbf{x}_i$ can be written in coordinates as (x_i, y_i); a pair of such $\mathbf{x}$ lie in $\mathbb{R}^2 \times \mathbb{R}^2$. Now consider applying the same affine transformation to each $\mathbf{x}$ independently: $\mathbf{x}_i \mapsto A\mathbf{x}_i + \mathbf{b}$ where $A \in GL(2, \mathbb{R})$ and $\mathbf{b} \in \mathbb{R}^2$. Then the Omega Process is a second-order differential operator defined by:

$$\Omega_{ij} = \begin{vmatrix} \frac{\partial}{\partial x_i} & \frac{\partial}{\partial y_i} \\ \frac{\partial}{\partial x_j} & \frac{\partial}{\partial y_j} \end{vmatrix} = \frac{\partial^2}{\partial x_i \partial y_j} - \frac{\partial^2}{\partial x_j \partial y_i}. \tag{8}$$

Under the above affine transformation, $\Omega_{ij} \mapsto (\det A)^{-1}\Omega_{ij}$, and is therefore a relative invariant. Note that $(\det A)^{-1}$ has no dependence on the coordinates. The Omega Process can be applied to products of pairs of smooth functions as follows, writing $\frac{\partial f}{\partial x}$ as f_x:

$$\Omega_{ij}\left(f(x_i, y_i)g(x_j, y_j)\right) = f_{x_i} g_{y_j} - f_{y_i} g_{x_j}. \tag{9}$$

Identifying $x_i = x_j = x, y_i = y_j = y$ gives functions of x and y that only vary by a scaling factor of $(\det A)^{-1}$ when $\mathbf{x}$ is mapped by an affine transformation. This matches the definition of a first-order partial transvectant of two functions:

$$\mathrm{tr}\Omega_{ij} f(x_i, y_i)g(x_j, y_j), \tag{10}$$

where tr is the operator that identifies the coordinates of each function $x_i = x_j = x, y_i = y_j = y$.

This can be generalised to n functions $f^{(1)}(x_1, y_1), \ldots, f^{(n)}(x_n, y_n)$ and r-th order [41] to define a partial transvectant as:

$$\mathrm{tr}\left[(\Pi_{k=1}^{r}\Omega_{i_k j_k})\, f^{(1)}(x_1, y_1) f^{(2)}(x_2, y_2), \ldots f^{(n)}(x_n, y_n)\right], \tag{11}$$

where $i_k \neq j_k \in \{1, \ldots, n\}$.

Under this formula there is a factor $(\det A)^{-r}$ in place of $(\det A)^{-1}$ that we saw previously, when all n copies of $\mathbb{R}^2$ are transformed by the same affine function $\mathbf{x} \mapsto A\mathbf{x} + \mathbf{b}$. Note that the individual pairwise Omega processes commute.

For the current case it is sufficient to consider n copies of the same function f. If we represent each copy of $\mathbb{R}^2$ as a node in an undirected graph, and each Omega process Ω_{ij} as an edge joining nodes i and j, a partial transvectant can be compactly represented in a graphical form. For example, consider a weight 2 transvectant defined as:

$$\begin{aligned}
&\mathrm{tr}\,[(\Omega_{12}\Omega_{12})f(x_1,y_1)f(x_2,y_2)] \\
&\quad = \mathrm{tr}\,[(\partial_{x_1y_2} - \partial_{x_2y_1})(\partial_{x_1y_2} - \partial_{x_2y_1})f(x_1,y_1)f(x_2,y_2)] \\
&\quad = \mathrm{tr}\,[(\partial_{x_1y_2} - \partial_{x_2y_1})\,(f_x(x_1,y_1)f_y(x_2,y_2) - f_y(x_1,y_1)f_x(x_2,y_2))] \\
&\quad = \mathrm{tr}2\,[f_{xx}(x_1,y_1)f_{yy}(x_2,y_2) - f_{xy}(x_1,y_1)f_{xy}(x_2,y_2)] \\
&\quad = 2f_{xx}(x,y)f_{yy}(x,y) - 2f_{xy}(x,y)^2.
\end{aligned}$$

This is a degree 2 partial transvectant as it involves derivatives of f up to second-order, and can be represented graphically by the following diagram:

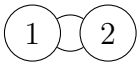

where the double edge corresponds to the two copies of Ω_{12} (the names are purely for convenience), i.e., the weight is the number of edges in the graph.

Tables 1 and 2 show all possible non-zero partial transvectants of A_2 up to weight 4 that can be generated in this way.

Owing to the group-subgroup structure some of these partial transvectants appear in signatures from other transformation groups, so for future reference, we define:

$$\begin{aligned}
C &= f_{xx}f_{yy} - f_{xy}^2, \\
D &= f_x^2 f_{yy} - 2f_x f_y f_{xy} + f_{xx}f_y^2, \\
E &= f_{xxx}f_y^3 - 3f_{xxy}f_x f_y^2 + 3f_{xyy}f_x^2 f_y - f_{yyy}f_x^3.
\end{aligned} \tag{12}$$

3.1. Signatures of $SA(2)$ and $A(2)$

The action of the affine group $A(2)$ arises in images as the motion of planar objects in images taken from a distant camera. Because $SA(2)$ is a subgroup of $A(2)$, any invariant of $A(2)$ is also an invariant of $SA(2)$, but not necessarily vice-versa. Any of the partial transvectants found in Tables 1 and 2 are invariants of $SA(2)$ as the determinant is 1. Hence, we can form a signature for $SA(2)$ by choosing any combination of partial transvectants. We choose a signature with three components so that it can be visualised as a three-dimensional surface; note that this will not be complete and may well have a very large bad set. For example, we can choose the function value together with C and D from Eq. (12) to form the signature:

$$\mathcal{I}_{SA(2)}(f) = (f, C, D)\,. \tag{13}$$

Fig. 6 shows the signature of our test image under an $SA(2)$ transformation.

For $A(2)$ the weight of the partial transvectants prevents them from being invariants. There are two options to create a signature. One is to select ratios of partial transvectants, as discussed in Section 2.3.

Degree	Weight	Diagram	Partial transvectant
2	2		$2f_{xx}f_{yy} - 2\left(f_{xy}\right)^2$
2	2	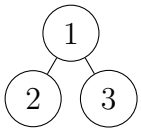	$\left(f_x\right)^2 f_{yy} - 2f_x f_y f_{xy} + f_{xx}\left(f_y\right)^2$
2	4	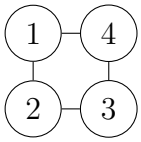	$2\left(f_{xx}\right)^2\left(f_{yy}\right)^2 - 4f_{xx}f_{yy}\left(f_{xy}\right)^2 + 2\left(f_{xy}\right)^4$
2	4	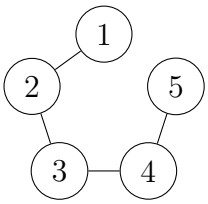	$\left(f_x\right)^2 f_{xx}\left(f_{yy}\right)^2 - \left(f_x\right)^2 f_{yy}\left(f_{xy}\right)^2$ $- 2f_x f_{xx} f_y f_{yy} f_{xy} + 2f_x f_y\left(f_{xy}\right)^3$ $+ \left(f_{xx}\right)^2\left(f_y\right)^2 f_{yy} - f_{xx}\left(f_y\right)^2\left(f_{xy}\right)^2$
3	3	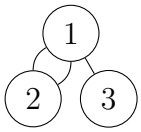	$-f_x f_{xx} f_{yyy} - f_x f_{yy} f_{xxy} + 2f_x f_{xy} f_{xyy}$ $+ f_{xx} f_y f_{xyy} + f_{xxx} f_y f_{yy} - 2f_y f_{xy} f_{xxy}$
3	3	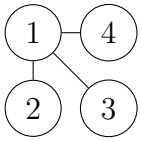	$-\left(f_x\right)^3 f_{yyy} + 3\left(f_x\right)^2 f_y f_{xyy} - 3f_x\left(f_y\right)^2 f_{xxy}$ $+ f_{xxx}\left(f_y\right)^3$
3	4	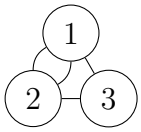	$2f_{xx}f_{yyy}f_{xxy} - 2f_{xx}\left(f_{xyy}\right)^2 + 2f_{xxx}f_{yy}f_{xyy}$ $- 2f_{xxx}f_{yyy}f_{xy} - 2f_{yy}\left(f_{xxy}\right)^2 + 2f_{xy}f_{xyy}f_{xxy}$
3	4	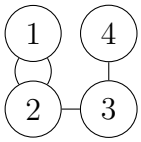	$-f_x f_{xx} f_{yy} f_{xyy} + f_x f_{xx} f_{yyy} f_{xy} - f_x f_{xxx}\left(f_{yy}\right)^2$ $+ 3f_x f_{yy} f_{xy} f_{xxy} - 2f_x\left(f_{xy}\right)^2 f_{xyy} - \left(f_{xx}\right)^2 f_y f_{yyy}$ $- f_{xx} f_y f_{yy} f_{xxy} + 3f_{xx} f_y f_{xy} f_{xyy}$ $+ f_{xxx} f_y f_{yy} f_{xy} - 2f_y\left(f_{xy}\right)^2 f_{xxy}$
3	4	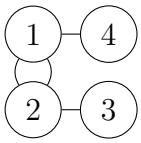	$2\left(f_x\right)^2 f_{yyy} f_{xxy} - 2\left(f_x\right)^2\left(f_{xyy}\right)^2$ $- 2f_x f_{xxx} f_y f_{yyy} + 2f_x f_y f_{xyy} f_{xxy}$ $+ 2f_{xxx}\left(f_y\right)^2 f_{xyy} - 2\left(f_y\right)^2\left(f_{xxy}\right)^2$
3	4	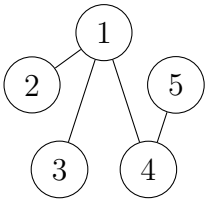	$-\left(f_x\right)^3 f_{yy} f_{xyy} + \left(f_x\right)^3 f_{yyy} f_{xy}$ $- \left(f_x\right)^2 f_{xx} f_y f_{yyy} + 2\left(f_x\right)^2 f_y f_{yy} f_{xxy}$ $- \left(f_x\right)^2 f_y f_{xy} f_{xyy} + 2f_x f_{xx}\left(f_y\right)^2 f_{xyy}$ $- f_x f_{xxx}\left(f_y\right)^2 f_{yy} - f_x\left(f_y\right)^2 f_{xy} f_{xxy}$ $- f_{xx}\left(f_y\right)^3 f_{xxy} + f_{xxx}\left(f_y\right)^3 f_{xy}$

Table 1: Details and graphical representations of all partial transvectants up to degree 3 of copies of a function f under a transformation in $A(2)$.

Degree	Weight	Diagram	Partial transvectant
4	4	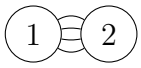	$f_{xxxx}f_{yyyy} - 4f_{xyyy}f_{xxxy} + 3f_{xxyy}^2$
4	4	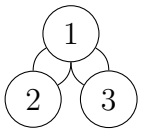	$f_{xx}^2 f_{yyyy} + 2f_{xx}f_{yy}f_{xxyy} - 4f_{xx}f_{xy}f_{xyyy} - 4f_{yy}f_{xy}f_{xxxy} + 4f_{xy}^2 f_{xxyy} + f_{xxxx}f_{yy}^2$
4	4	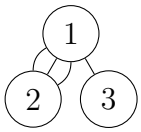	$f_x f_{xxx} f_{yyyy} - f_x f_{yyy} f_{xxxy} + 3f_x f_{xyy} f_{xxyy} - 3f_x f_{xyyy} f_{xxy} - f_{xxx} f_y f_{xyyy} + f_{xxxx} f_y f_{yyy} - 3f_y f_{xyy} f_{xxxy} + 3f_y f_{xxy} f_{xxyy}$
4-4	4	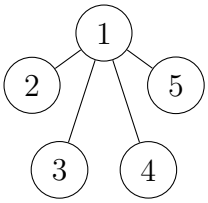	$(f_x)^4 f_{yyyy} - 4(f_x)^3 f_y f_{xyyy} + 6(f_x)^2 (f_y)^2 f_{xxyy} - 4f_x (f_y)^3 f_{xxxy} + f_{xxxx} (f_y)^4$

Table 2: Details and graphical representations of all partial transvectants of weight 4 of copies of a function f under a transformation in $A(2)$.

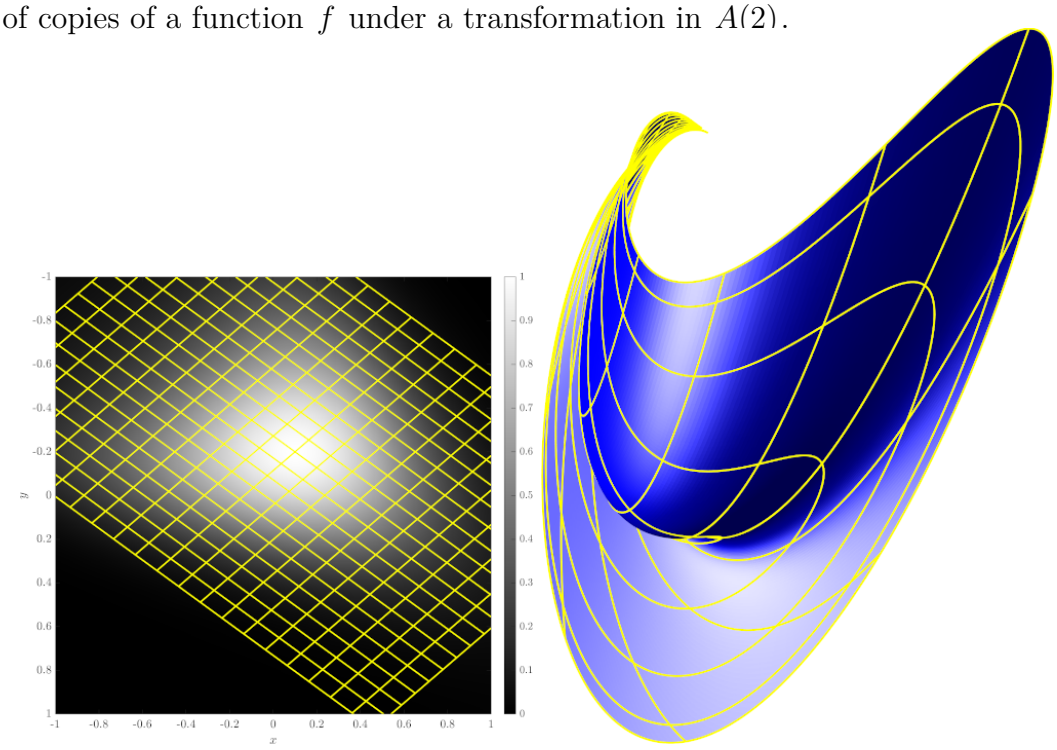

Figure 6: A sample $SA(2)$ transformation applied to our test function, and the corresponding signature.

It is then beneficial to choose the numerator and denominator so that they have different critical points, which can be achieved by adding together partial transvectants of the same weight as appropriate. Instead, we employ the same normalisation strategy as previously, projecting the weight four relative invariants (C^2, D^2, E) onto the unit hypersphere and multiplying by f. In this way, our signature is:

$$\mathcal{I}_{A(2)} = \frac{f}{\sqrt{C^4 + D^4 + E^2}}(C^2, D^2, E) \tag{14}$$

We will subject our test image to the special affine transformation: Fig. 7 shows the signature of our test image under this transformation.

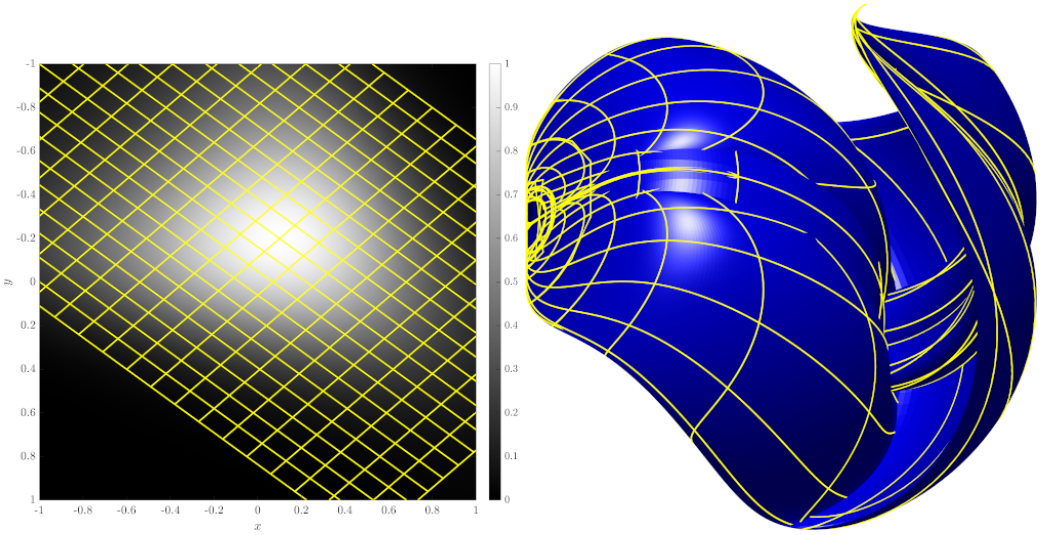

Figure 7: A sample $A(2)$ transformation applied to our test function, and the corresponding signature.

4. Differential invariants through moving frames

So far, the methods that we have seen to construct differential invariants for particular groups are not directly generalisable. It is natural to ask if there is an algorithmic approach that will yield invariants more directly. The answer is a qualified yes. There is a general method, based on Cartan's method of moving frames, that is generally applicable, but finding good solutions with it still requires some ingenuity in general. Olver and co-authors have developed [14] and popularised the approach, and made it applicable to object recognition based on outline curves, see [44] for an overview, and note particularly the original application paper [6]. We introduce the method here and then demonstrate its use to find invariants to further groups, but for further technical details see [42].

A moving frame is a mapping into a group $\mathcal{G}$ that provides a frame of reference along a manifold. It was used by [7] as the basis for his 'method of moving frames', which uses Cartan equivalence to identify the set of structural invariants of a manifold. [13, 14] showed that the actions of a Lie group $\mathcal{G}$ enable the identification of invariants to that group through the definition of a $\mathcal{G}$-equivariant mapping.

A (right-) moving frame is a smooth $\mathcal{G}$-equivariant map $\rho : \mathcal{M} \to \mathcal{G}$ such that $\rho(g \cdot z) = \rho(z) \cdot g^{-1}$, where $z \in J^d$ and where "$\cdot$" denotes the group operation of $\mathcal{G}$. It is necessary [43] for the group to act freely. This means that the group action needs to be extended to the entire jet space of derivatives up to order d by implicit differentiation of the group action, a process known as prolongation.

The procedure to construct differential invariants to the action of Lie group $\mathcal{G}$ acting on manifold $\mathcal{M}$ using the method of moving frames is as follows:

1. Prolong the group action to the jet space of d-th order derivatives J^d.

2. Apply Cartan normalisation:
   (a) Choose a local cross-section to the group orbits, i.e., a $(d - \dim \mathcal{G})$-dimensional submanifold $\mathcal{K}$ that intersects transversally at most once with each orbit
   (b) $\mathcal{K}$ is specified by $\dim \mathcal{G}$ independent equations $Z_i(z) = c_i$, for $z \in J^d$, and Z_i scalar-valued functions and c_i constants.
   (c) The right-moving frame $g = \rho(z)$ is found by solving the normalisation questions $Z_i(g \cdot z) = c_i$ for the group parameters g (in terms of z). In other words, the moving frame is the transformation back to the cross-section.
3. The differential invariants are not affected by the action of the group: $I(g \cdot z) = I(z)\ \forall z \in \mathrm{dom} I$, or equivalently, are constant on the orbits.

Cartan normalisation can be considered as identifying a canonical subspace (with some coordinates fixed) in the jet space to which any point in the jet space can be mapped by a group action.

[42] uses the group $SE(2)$ on curves as an example, recovering the Euclidean curvature as a second-order invariant. We continue this example to compute invariants to $SE(2)$ for images, before moving on to other planar Lie group examples: $E(2)$, the Möbius group ($PSL(2, \mathbb{C})$) and the projective group ($PSL(3, \mathbb{R})$). Finally, we apply the method to an infinite-dimensional pseudo-Lie group, the conformal diffeomorphisms.

4.1. The special Euclidean group SE(2)

An element of the special Euclidean group $SE(2)$ acts on an element (x, y) of $\mathbb{R}^2$ to produce $(\bar{x}, \bar{y})$ as:

$$\bar{x} = x \cos\theta - y \sin\theta + t_x \quad \text{and} \quad \bar{y} = x \sin\theta + y \cos\theta + t_y.$$

We prolong the group action to form the jet space J^2 with coordinates $(x, y, f, f_x, f_y, f_{xx}, f_{xy}, f_{yy})$ via the chain rule. The transformation rule for the derivatives is given by:

$$\begin{bmatrix} \bar{f}_{\bar{x}} \\ \bar{f}_{\bar{y}} \\ \bar{f}_{\bar{x}\bar{x}} \\ \bar{f}_{\bar{x}\bar{y}} \\ \bar{f}_{\bar{y}\bar{y}} \end{bmatrix} = \begin{bmatrix} c & -s & 0 & 0 & 0 \\ s & c & 0 & 0 & 0 \\ 0 & 0 & c^2 & -2cs & s^2 \\ 0 & 0 & cs & c^2 - s^2 & -cs \\ 0 & 0 & s^2 & 2cs & c^2 \end{bmatrix} \begin{bmatrix} f_x \\ f_y \\ f_{xx} \\ f_{xy} \\ f_{yy} \end{bmatrix}, \tag{15}$$

where $c = \cos\theta$ and $s = \sin\theta$. Because the group has three parameters, we choose the cross-section of the group orbits to be $\bar{x} = 0, \bar{y} = 0, \bar{f}_{\bar{y}} = 0$. We also require that $\bar{f}_{\bar{x}} > 0$ to uniquely define the moving frame. Note that the group action is locally free (away from critical points) when prolonged to J^1, however we prolong to J^2 in order to compute invariants. The moving frame is then given by the prolonged Euclidean transformation that maps an element of J^2 to this cross-section. It can be thought of as rotating the image about that point so that its gradient is pointing in the positive x direction, and then translating the image so the point is mapped to the origin.

This choice of moving frame gives $\cos\theta = f_x/\|\nabla f\|$ and $\sin\theta = -f_y/\|\nabla f\|$. The parameters t_x, t_y are then $t_x = -x\cos\theta + y\sin\theta$ and $t_y = -x\sin\theta - y\cos\theta$, however these have no effect on the derivatives, and will henceforth be ignored.

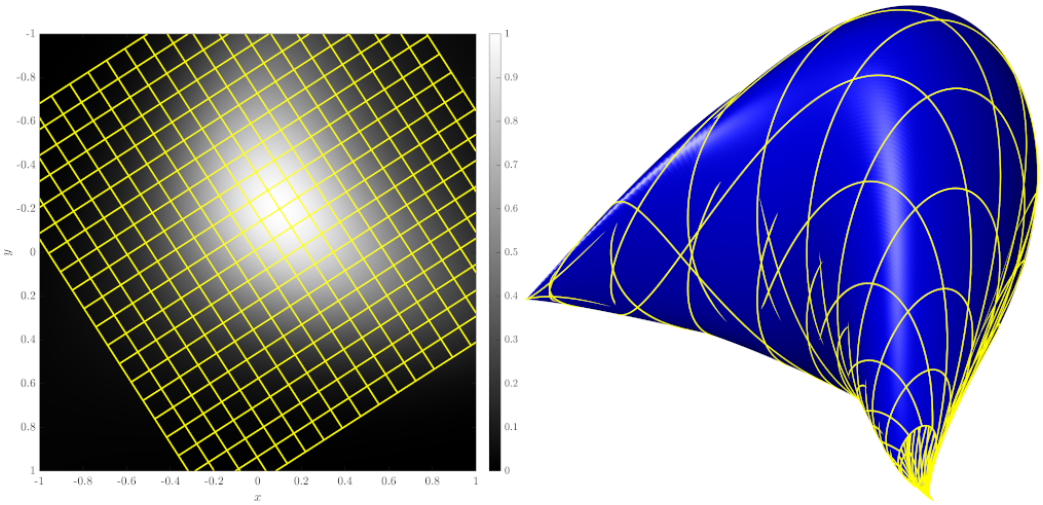

Figure 8: A sample $SE(2)$ transform and 3D signature.

The remaining elements not fixed by the cross-section, $\bar{f}$, $\bar{f}_{\bar{x}}$, $\bar{f}_{\bar{x}\bar{x}}$, $\bar{f}_{\bar{x}\bar{y}}$, and $\bar{f}_{\bar{y}\bar{y}}$, are therefore all invariant. This gives the following set of invariants:

$$\begin{aligned}
K_0 &= f \\
K_1 &= f_x^2 + f_y^2 && (= \bar{f}_{\bar{x}}^2) \\
K_2 &= f_x^2 f_{xx} + 2 f_x f_y f_{xy} + f_y^2 f_{yy} && (= K_1 \bar{f}_{\bar{x}\bar{x}}) \\
K_3 &= f_x f_y (f_{yy} - f_{xx}) + f_{xy}(f_x^2 - f_y^2) && (= K_1 \bar{f}_{\bar{x}\bar{y}}) \\
K_4 &= f_y^2 f_{xx} - 2 f_x f_y f_{xy} + f_x^2 f_{yy} && (= K_1 \bar{f}_{\bar{y}\bar{y}}).
\end{aligned} \tag{16}$$

Note that we have multiplied each of the second derivative invariants by the invariant K_1 so that they decay smoothly to zero at critical points. Interestingly, K_4 is the affine invariant D from Eq. (12) and K_1 and K_2 are also Euclidean invariants, so we need to include K_3 in our signature:

$$I_{SE(2)}(f) = (f, K_1, K_3). \tag{17}$$

Fig. 8 shows the signature of our test image under a sample transformation of $SE(2)$.

4.2. The Euclidean group E(2)

An element of the Euclidean group $E(2)$ maps an element (x, y) of $\mathbb{R}^2$ to $(\bar{x}, \bar{y})$ as:

$$\bar{x} = x\varepsilon\cos\theta - y\varepsilon\sin\theta + t_x \quad \text{and} \quad \bar{y} = x\sin\theta + y\cos\theta + t_y.$$

where $\varepsilon \in \{-1, 1\}$ and the remaining parameters are the same as for $SE(2)$. If $\varepsilon = 1$ it is a rigid transformation, and if $\varepsilon = -1$ it contains a reflection.

This time, the group action is not free on J^1 (with elements of the form (x, y, f, f_x, f_y)) away from critical points because there are two possible transformations that map to the cross-section $(0, 0, \bar{f}, \bar{f}_{\bar{x}}, 0)$ where $\bar{f}_{\bar{x}} > 0$, one that reflects the gradient into the positive x direction, and one that rotates.

We again prolong the group action to J^2, but this time we expect to need to use a second derivative term to determine ε for the moving frame. The derivative transformations are given by:

$$\begin{bmatrix} \bar{f}_{\bar{x}} \\ \bar{f}_{\bar{y}} \\ \bar{f}_{\bar{x}\bar{x}} \\ \bar{f}_{\bar{x}\bar{y}} \\ \bar{f}_{\bar{y}\bar{y}} \end{bmatrix} = \begin{bmatrix} \varepsilon c & -\varepsilon s & 0 & 0 & 0 \\ s & c & 0 & 0 & 0 \\ 0 & 0 & c^2 & -2cs & s^2 \\ 0 & 0 & \varepsilon cs & \varepsilon(c^2 - s^2) & -\varepsilon cs \\ 0 & 0 & s^2 & 2cs & c^2 \end{bmatrix} \begin{bmatrix} f_x \\ f_y \\ f_{xx} \\ f_{xy} \\ f_{yy} \end{bmatrix}, \tag{18}$$

where again $c = \cos\theta$ and $s = \sin\theta$.

We begin by choosing the same cross-section as for $SE(2)$, namely $\bar{x} = 0$, $\bar{y} = 0$, $\bar{f}_{\bar{y}} = 0$, $\bar{f}_{\bar{x}} > 0$. This gives $\cos\theta = \varepsilon f_x / \|\nabla f\|$ and $\sin\theta = -\varepsilon f_y / \|\nabla f\|$. Under this transformation, regardless of whether $\varepsilon = 1$ or $\varepsilon = -1$, the derivative $\bar{f}_{\bar{x}} = \|\nabla f\|$. The only second derivative term in which ε appears is the $\bar{f}_{\bar{x}\bar{y}}$ term, so we use this to resolve the sign. Substituting in for $\cos\theta, \sin\theta$, we see that:

$$\bar{f}_{\bar{x}\bar{y}} = \frac{\varepsilon(f_x f_y(f_{yy} - f_{xx}) + (f_x^2 - f_y^2) f_{xy})}{f_x^2 + f_y^2}.$$

This suggests choosing ε to make $\bar{f}_{\bar{x}\bar{y}} \geq 0$. The moving frame is then fully specified, and the remaining derivatives give the same invariants K_0, K_1, K_2, K_4 as for $SE(2)$, (16), the one difference being:

$$\hat{K}_3 = |f_x f_y(f_{yy} - f_{xx}) + f_{xy}(f_x^2 - f_y^2)| \tag{19}$$

These invariants are a functionally independent, complete, set of polynomial differential invariants up to second derivatives. Note that the invariants found previously by tensor contraction Eq. (5) in Section 2.2 can be expressed in terms of them (see the replacement theorem in [14] for a justification of this):

$$f = f = K_0, \quad f_i f_i = f_x^2 + f_y^2 = K_1$$
$$f_{ii} = f_{xx} + f_{yy} = \frac{K_2 + K_4}{K_1}, \quad f_{ij} f_{ij} = f_{xx}^2 + 2f_{xy}^2 + f_{yy}^2 = \frac{K_2^2 + K_4^2 + 2K_3^2}{K_1^2}$$
$$f_i f_j f_{ij} = f_x^2 f_{xx} + 2 f_x f_y f_{xy} + f_y^2 f_{yy} = K_2.$$

4.3. The Möbius group

The Möbius group $PSL(2, \mathbb{C})$ acts on the Riemann sphere $\overline{\mathbb{C}} = \mathbb{C} \cup \infty$ by:

$$\phi \colon \overline{\mathbb{C}} \to \overline{\mathbb{C}}, \quad \phi(z) = \frac{\alpha z + \beta}{\gamma z + \delta}, \quad \alpha, \beta, \gamma, \delta \in \mathbb{C}, \quad \alpha\delta - \beta\gamma \neq 0. \tag{20}$$

Identifying $\mathbb{R}^2$ with $\mathbb{C}$, the Möbius group is a real 6-dimensional local Lie group acting on $\mathbb{R}^2$. It is the smallest nonlinear planar group that contains $SE(2)$, and it also has direct applications in image processing since it arises in the *conformal camera* model of vision, in which scenes are projected radially onto a sphere [32, 55]; it is also the set of biholomorphic maps of the Riemann sphere.

We are free to take $\delta = 1$. Then $\bar{f} = f$ means that z is translated to β; we can therefore take $\beta = 0$. This leaves 4 group parameters a, b, c, d, where $\alpha = a + ib$,

$\gamma = c + id$, to be determined as follows. We prolong the action to second derivatives of f, which is sufficient to allow the group to act freely. There are 5 derivatives of f up to order 2, so there will be at least 1 invariant. In order to find further invariants the prolongation to 3rd derivatives is required, which will result in at least another four invariants. This simple counting argument works because the group acts freely on the prolongation. The prolonged action is:

$$\begin{bmatrix} \bar{f}_{\bar{x}} \\ \bar{f}_{\bar{y}} \\ \bar{f}_{\bar{x}\bar{x}} \\ \bar{f}_{\bar{x}\bar{y}} \\ \bar{f}_{\bar{y}\bar{y}} \end{bmatrix} = \begin{bmatrix} a & b & 0 & 0 & 0 \\ -b & a & 0 & 0 & 0 \\ 2\mu & -2\rho & a^2 & 2ab & b^2 \\ 2\rho & 2\mu & -ab & a^2 - b^2 & ab \\ -2\mu & 2\rho & b^2 & -2ab & a^2 \end{bmatrix} \begin{bmatrix} f_x \\ f_y \\ f_{xx} \\ f_{xy} \\ f_{yy} \end{bmatrix}. \tag{21}$$

where $\mu = bd - ac$ and $\rho = bc + ad$. The moving frame calculation is then:

1. The partial cross-section $\bar{f}_{\bar{x}} = 1$, $\bar{f}_{\bar{y}} = 0$ determines two group parameters:
$$a = f_x/(f_x^2 + f_y^2), \quad b = f_y/(f_x^2 f_y^2).$$
2. The partial cross-section $\bar{f}_{\bar{x}\bar{y}} = \bar{f}_{\bar{y}\bar{y}} = 0$ determines the next group parameters:
$$c = (2f_x f_y f_{xyy} - f_{xx} f_y^2 - f_{yy} f_x^2)/(2f_x^2 + f_y^2)^2$$
$$d = (f_{xy} f_x^2 - f_x f_y f_{xx} - f_{xy} f_y^2 - f_{yy} f_x f_y)/(2f_x^2 + f_y^2)^2.$$
3. The second-order invariant is then given by $\bar{f}_{\bar{x}\bar{x}}$ using Eq. (21):
$$\bar{f}_{\bar{x}\bar{x}} = \frac{f_{xx} + f_{yy}}{f_x^2 + f_y^2}.$$

The four third-order invariants can be deduced from the moving frame. They are rational functions with numerators of degree 6 and denominators $(f_x^2 + f_y^2)^4$, and are relative invariants of weight 8. Clearing denominators so as to work with polynomials, we choose $M_1 = (f_{xx} + f_{yy})^4$ and two of the four third-order invariants M_2 and M_3:

$$\begin{aligned} M_2 = {} & f_y^5 f_{yyy} + \tfrac{9}{2} f_y^2 f_{yy}^2 f_x^2 + f_y^3 f_{yyy} f_x^2 + \tfrac{3}{2} f_{yy}^2 f_x^4 - 9 f_y^3 f_{yy} f_x f_{xy} + 3 f_y f_{yy} f_x^3 f_{xy} \\ & + \tfrac{3}{2} f_y^4 f_{xy}^2 - 9 f_y^2 f_x^2 f_{xy}^2 + \tfrac{3}{2} f_z^4 f_{xy}^2 + 3 f_y^4 f_x f_{xyy} + 3 f_y^2 f_x^3 f_{xyy} + 3 f_y^4 f_{yy} f_{xx} \\ & + 3 f_{yy} f_x^4 f_{xx} + 3 f_y^3 f_x f_{xy} f_{xx} - 9 f_y f_x^3 f_{xy} f_{xx} + \tfrac{3}{2} f_y^4 f_{xx}^2 + \tfrac{9}{2} f_y^2 f_x^2 f_{xx}^2 + 3 f_y^3 f_x^2 f_{xxy} \\ & + 3 f_y f_x^4 f_{xxy} + f_y^2 f_x^3 f_{xxx} + f_x^5 f_{xxx}, \end{aligned}$$

$$\begin{aligned} M_3 = {} & -3 f_y f_{yy}^2 f_x^3 + f_y^2 f_{yyy} f_x^3 + f_{yyy} f_x^5 + 9 f_y^2 f_{yy} f_x^2 f_{xy} - 3 f_{yy} f_x^4 f_{xy} - 6 f_y^3 f_x f_{xy}^2 \\ & + 6 f_y f_x^3 f_{xy}^2 - 3 f_y^3 f_x^2 f_{xyy} - 3 f_y f_x^4 f_{xyy} - 3 f_y^3 f_{yy} f_x f_{xx} + 3 f_y f_{yy} f_x^3 f_{xx} \\ & + 3 f_y^4 f_{xy} f_{xx} - 9 f_y^2 f_x^2 f_{xy} f_{xx} + 3 f_y^3 f_x f_{xx}^2 + 3 f_y^4 f_x f_{xxy} + 3 f_y^2 f_x^3 f_{xxy} \\ & - f_y^5 f_{xxx} - f_y^3 f_x^2 f_{xxx}. \end{aligned}$$

We then form a signature by our usual projection method from the image f and these three weight 8 relative invariants:

$$\mathcal{I}_{\text{Möbius}}(f) = \frac{f}{\sqrt{M_1^2 + M_2^2 + M_3^2}}(M_1, M_2, M_3) \tag{22}$$

An example is shown in Fig. 9, although note that the signature is singular when $f_x = f_y = f_{xx} + f_{yy} = 0$, a codimension 1 phenomenon for images.

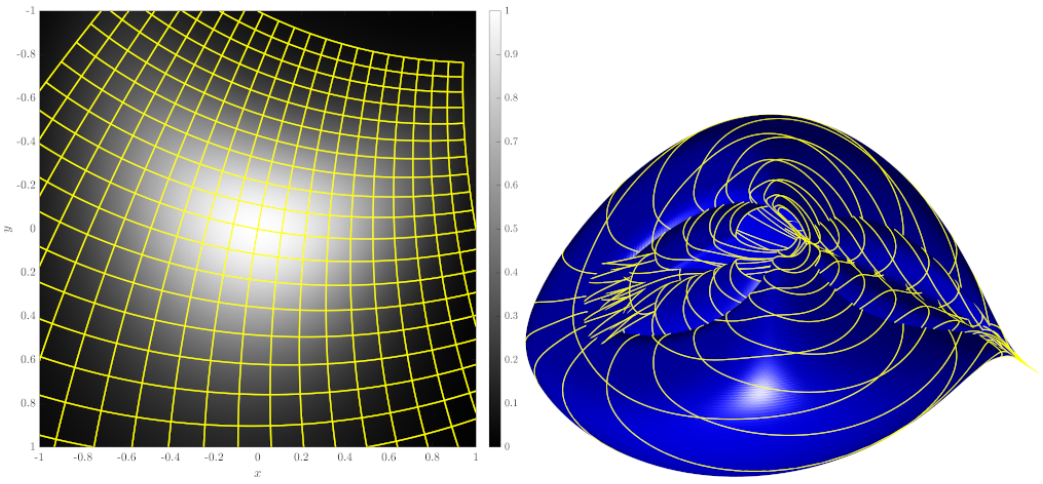

Figure 9: A sample Möbius transform and 3D signature.

4.4. The projective group

The action of the projective group arises naturally through the movements of the camera viewing planar objects. We consider the eight-dimensional group $PSL(3,\mathbb{R})$ acting on $\mathbb{R}^2$ by projective transformations, i.e.,

$$(x, y) \mapsto \left(\frac{ax + by + j}{l + gx + hy}, \frac{cx + dy + k}{l + gx + hy} \right). \tag{23}$$

Requiring that $\bar{f} = f$ enables us to clear the translation coefficients, so $j = k = 0$; for convenience we will also take $l = 1$. This leaves 6 group parameters (a, b, c, d, g, h) to be determined. For free action it is necessary to prolong the group action to 3rd derivatives of f. Since there are 9 derivatives of f of order 1, 2, and 3, there will be at least 3 invariants. The prolonged action is:

$$\begin{bmatrix} \bar{f}_{\bar{x}} \\ \bar{f}_{\bar{y}} \\ \bar{f}_{\bar{x}\bar{x}} \\ \bar{f}_{\bar{x}\bar{y}} \\ \bar{f}_{\bar{y}\bar{y}} \\ \bar{f}_{\bar{x}\bar{x}\bar{x}} \\ \bar{f}_{\bar{x}\bar{x}\bar{y}} \\ \bar{f}_{\bar{x}\bar{y}\bar{y}} \\ \bar{f}_{\bar{y}\bar{y}\bar{y}} \end{bmatrix} = \begin{bmatrix} a & c & 0 & 0 & 0 & 0 & 0 & 0 & 0 \\ b & d & 0 & 0 & 0 & 0 & 0 & 0 & 0 \\ -2ag & -2cg & a^2 & 2ac & c^2 & 0 & 0 & 0 & 0 \\ -bg-ah & -dg-ch & ab & bc+ad & cd & 0 & 0 & 0 & 0 \\ -2bh & -2dh & b^2 & 2bd & d^2 & 0 & 0 & 0 & 0 \\ 6ag^2 & 6cg^2 & -6a^2g & -12acg & -6c^2g & a^3 & 3a^2c & 3ac^2 & c^3 \\ 2g\alpha_1 & 2g\beta_1 & -2a\alpha_2 & -4\delta_1 & -2c\beta_2 & a^2b & a\gamma_1 & c\gamma_1 & c^2d \\ 2h\alpha_2 & 2h\beta_2 & -2b\alpha_1 & -4\delta_2 & -2d\beta_1 & ab^2 & b\gamma_1 & d\gamma_2 & cd^2 \\ 6bh^2 & 6dh^2 & -6b^2h & -12bdh & -6d^2h & b^3 & 3b^2d & 3bd^2 & d^3 \end{bmatrix} \begin{bmatrix} f_x \\ f_y \\ f_{xx} \\ f_{xy} \\ f_{yy} \\ f_{xxx} \\ f_{xxy} \\ f_{xyy} \\ f_{yyy} \end{bmatrix}. \tag{24}$$

where $\alpha_1 = bg + 2ah$, $\alpha_2 = 2bg + ah$, $\beta_1 = dg + 2ch$, $\beta_2 = 2dg + ch$, $\gamma_1 = bc + 2ad$, $\gamma_2 = 2bc + ad$, and $\delta_1 = (bcg + adg + ach)$, $\delta_2 = (bdg + bch + adh)$.

We begin the construction of the moving frame by choosing $\bar{f}_{\bar{x}} = 1$ and $\bar{f}_{\bar{y}} = 0$, which determines the group parameters $a = (1 - cf_y)/f_x$. and $b = -df_y/f_x$. Direct substition then shows that $\bar{f}_{\bar{y}\bar{y}} = Dd^2/f_x^2$, where $D = f_x^2 f_{yy} + f_y^2 f_{xx} - 2f_x f_y f_{xyy}$ was listed in Eq. (12) as an invariant of $A(2)$, which is a subgroup of $PSL(3,\mathbb{R})$. Note that D and $\bar{f}_{\bar{y}\bar{y}}$ have the same sign. If $D < 0$, we choose the frame $\bar{f}_{\bar{y}\bar{y}} = -1$ and if $D \geq 0$ we choose $\bar{f}_{\bar{y}\bar{y}} = 1$. Then $d = f_x/|D|^{1/2}$.

The partial cross-section $\bar{f}_{\bar{y}\bar{y}\bar{y}} = 0$ determines the group parameter

$$h = \frac{f_{yyy}f_x^3 - 3f_x^2 f_y f_{xyy} + 3f_x f_y^2 f_{xxy} - f_y^3 f_{xxx}}{6|D|^{3/2}},$$

while $\bar{f}_{\bar{x}\bar{y}y} = 0$ provides us with $c = \frac{hf_x^2}{dD} - \frac{f_x f_{xy} - f_y f_{xx}}{D}$, and $\bar{f}_{\bar{x}\bar{x}} = 0$ finally leads to $g = \frac{1}{2f_x^2}(f_{xx} + 2c(f_x f_{xy} - f_y f_{xx}) + c^2 D)$. In fact, the numerator of the expression for h was another invariant of $A(2)$ labelled as E in Eq. (12).

Having determined the frame, any function of the remaining derivatives $\bar{f}_{\bar{x}\bar{x}\bar{x}}$, $\bar{f}_{\bar{x}\bar{x}\bar{y}}$, and $\bar{f}_{\bar{y}\bar{y}\bar{y}}$, as given in Eq. (24), provides invariants. We choose:

$$(\bar{f}_{\bar{x}\bar{x}\bar{x}}, \bar{f}^2_{\bar{x}\bar{x}\bar{y}}, \bar{f}_{\bar{x}\bar{y}\bar{y}}) = \left(\frac{J_1}{D^6}, \frac{J_2}{D^9}, \frac{J_3}{D^3}\right).$$

The terms J_1, J_2, J_3 can be written in terms of D and E, together with a polynomial of degree n denoted by P_n.

$$J_1 = E^4 + DP_{13}, \quad J_2 = (E^3 + DP_9)^2, \quad J_3 = E^2 - 12DP_5.$$

The J_i are polynomials of degree 16, 24, and 8, respectively, and are extremely complicated when written out explicitly. They do have one benefit, though, which is that they all have denominators given by integer powers of D, resolving the ambiguity caused by the sign of D. Therefore, $(D^{18}, J_1^3, J_2^2, J_3^6)$ are all relative invariants of weight 36, and so projecting any subset of them of them to a sphere yields a third-order invariant signature.

J vanishes on generic images: $J = 0$ when $D = E = 0$, which is a codimension 0 phenomenon for images. In particular, $D = E = 0$ at critical points. However, these signatures can be simplified and made more robust. Their structure suggests considering the combination $J_1 - J_3^2$, which obeys:

$$J_1 - J_3^2 = 144D^4 P_4.$$

As J_1/D^6 and J_3/D^3 are invariant, so is P_4/D^2. Moreover, the numerator of this new invariant does not vanish at critical points. It has the structure:

$$P_4 = -4(\det f_{ij})^2 + Q_4,$$

where Q_4 is a polynomial of degree 4 that vanishes when $f_x = f_y = 0$. Hence, the relative invariant signature of weight 12 $(D^6, P_4^3, (E^2 - 12DP_5)^2)$ can be projected to S^2, yielding a projective invariant of images that is singular only when $D = E = P_4 = 0$, which is a codimension 1 phenomenon, since $D = E = 0 \Rightarrow P_4 = 0$. In particular, at critical points it tends to $(0, (2\det f_{ij})^6, 0)$, and hence critical points with $\det f_{ij} \neq 0$ have signature value $(0, 1, 0)$. Including J_2 provides a 4-dimensional signature set, but does not change the codimension of the set of bad images.

4.5. Conformal diffeomorphisms $\mathbf{Diff_{con}}$

The conformal camera model is well known. The group of conformal diffeomorphisms is the subgroup of diffeomorphisms (i.e., smooth functions with smooth inverses) that are angle-preserving:

$$\angle(u, v) = \angle(D\phi(x).u, D\phi(x).v), \tag{25}$$

where $\angle(u, v)$ denotes the angle between tangent vectors u and v based at $x \in \mathbb{R}^2$, $\phi \in \text{Diff}$ and D represents the Jacobian. The group is infinite-dimensional, but still small enough that images have local differential invariants.

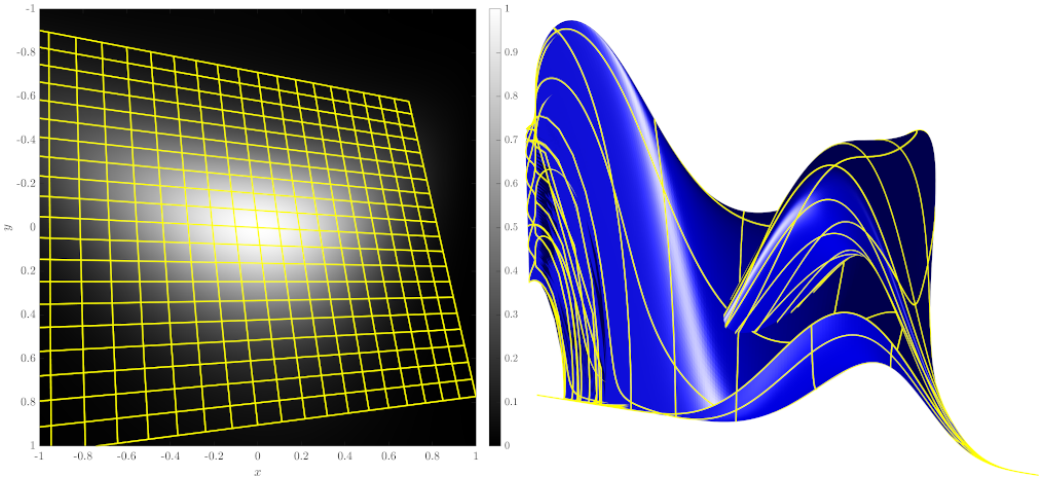

Figure 10: A sample $PSL(3, \mathbb{R})$ transform and 3D signature.

The conformal diffeomorphisms provides a particularly nice example of the moving frame method. Because the group is infinite dimensional, we need to prolong the group action to the infinite jet space J^∞ with elements of the form $(x, y, f, f_x, f_y, f_{xx}, f_{xy}, f_{yy}, \ldots)$.

It is convenient to work in the complex variable $z = x + iy$. Without loss of generality, we can assume $x = y = 0$. We begin the construction of our cross-section by choosing $\bar{x} = \bar{y} = 0$. Then ψ^{-1} can be represented locally by a Taylor series of the form:

$$z = \psi^{-1}(\bar{z}) = c_1\bar{z} + c_2\bar{z}^2 + c_3\bar{z}^3 + \cdots,$$

where $c_k = a_k + ib_k, k = 1, 2, \ldots$. We solve for the parameters a_k, b_k in stages. To find $c_1 = a_1 + ib_1$ we need two constraints. Differentiating $f(x, y) = \bar{f}(\bar{x}, \bar{y})$ and substituting in our existing cross-section constraints $\bar{x} = \bar{y} = 0$ gives:

$$\bar{f}_{\bar{x}} = f_x x_{\bar{x}} + f_y y_{\bar{x}} = a_1 f_x + b_1 f_y, \quad \text{and} \quad \bar{f}_{\bar{y}} = f_x x_{\bar{y}} + f_y y_{\bar{y}} = -b_1 f_x + a_1 f_y.$$

Note that $\bar{x} = \bar{y} = 0$ removes all higher order derivatives from the cross-section equation. Adding two extra constraints to the cross section, $\bar{f}_{\bar{x}} = 1, \bar{f}_{\bar{y}} = 0$, this system is readily solved to give:

$$a_1 = f_x/(f_x^2 + f_y^2), \quad b_1 = f_y/(f_x^2 + f_y^2).$$

We then repeat the process, this time using the second derivative computations. There are two new parameters, a_2, b_2, to solve for, but there are three derivatives. We use the cross-section equations $\bar{f}_{\bar{x}\bar{x}} = 0, \bar{f}_{\bar{x}\bar{y}} = 0$ to solve for a_2 and b_2, the remaining derivative $\bar{f}_{\bar{y}\bar{y}}$ is then the sole second-order invariant, which we also saw for the Möbius group:

$$\bar{f}_{\bar{y}\bar{y}} = \frac{f_{xx} + f_{yy}}{f_x^2 + f_y^2} = \frac{C_1}{f_x^2 + f_y^2}. \tag{26}$$

Continuing in this way, at derivative order n two real group parameters enter: a_n and b_n. There are $n + 1$ independent derivatives of f of order n, so there must be

$n-1$ new independent invariants at each order. Hence at third order there are two more invariants, using the constraints $\bar{f}_{\bar{x}\bar{x}\bar{x}} = 0, \bar{f}_{\bar{x}\bar{x}\bar{y}} = 0$, the remaining derivatives are invariant:

$$\begin{aligned}\bar{f}_{\bar{x}\bar{y}\bar{y}} &= \frac{1}{(f_x^2+f_y^2)^3}\Big[f_y^3 f_{yyy}+f_x^2 f_y f_{yyy}-2f_y^2 f_{yy}^2-2f_{xx}f_y^2 f_{yy}-2f_x^2 f_{xx}f_{yy}-4f_x f_{xy}f_y f_{yy}\\ &\quad + f_{xxy}f_y^3 + f_x^2 f_{xxy}f_y - 4f_x f_{xy}f_{xx}f_y + f_x^3 f_{xxx} - 2f_x^2 f_{xx}^2 + f_x^3 f_{xyy}\Big]\\ &= \frac{C_2}{(f_x^2+f_y^2)^3} \qquad (27)\\ \bar{f}_{\bar{y}\bar{y}\bar{y}} &= \frac{1}{(f_x^2+f_y^2)^3}\Big[f_x f_y^2 f_{yyy} + f_x^3 f_{yyy} - 2f_x f_y f_{yy}^2 + 2f_{xy}f_y^2 f_{yy} - 2f_x^2 f_{xy}f_{yy}\\ &\quad - f_{xxx}f_y^3 - f_{xyy}f_y^3 + f_x f_{xxy}f_y^2 + 2f_{xy}f_{xx}f_y^2 - f_x^2 f_{xxx}f_y + 2f_x f_{xx}^2 f_y\\ &\quad - f_x^2 f_{xyy}f_y + f_x^3 f_{xxy} - 2f_x^2 f_{xy}f_{xx}\Big] = \frac{C_3}{(f_x^2+f_y^2)^3} \qquad (28)\end{aligned}$$

Note that the denominators of all three of these equations are the same up to index. We therefore clear denominators as usual and form the signature using our usual projection technique:

$$\mathcal{I}_{\mathrm{Diff}_{\mathrm{con}}}(f) = \frac{f}{\sqrt{C_1^6+C_2^2+C_3^2}}(C_1^3, C_2, C_3) \qquad (29)$$

This signature is continuous at all (x, y) such that the three quantities are not simultaneously equal to zero, which occurs when $f_x = f_y = f_{xx} = f_{yy} = 0$, which is a codimension 1 phenomenon for images.

An example for the conformal map φ defined through φ^{-1} by $\varphi^{-1}(z) = \frac{3}{8}(z-2)^2 - \frac{3}{2}$ is shown in Fig. 11.

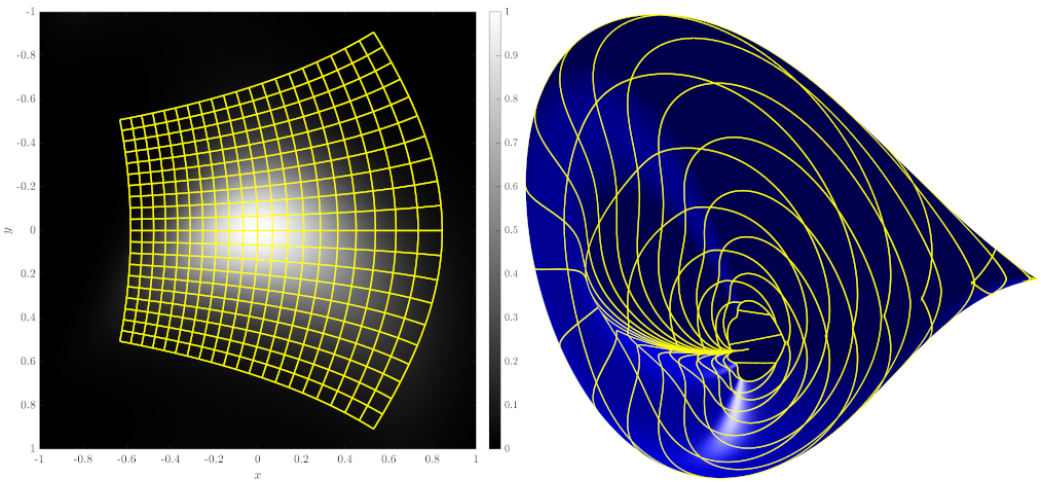

Figure 11: A sample Diff_{con} transform and 3D signature.

4.6. $\mathrm{Diff}_{\mathrm{vol}}$ and Diff

Two other infinite-dimensional groups are of interest: the volume-preserving diffeomorphisms, which act as the space of transformations of an incompressible fluid, and the full group of planar diffeomorphisms, which are widely-used in image registration [61]. However, in these cases there are no differential invariant signatures of greyscale images.

The volume-preserving diffeomorphisms $\mathrm{Diff}_{\mathrm{vol}}$ are those diffeomorphisms that preserve the volume form (area form in 2D). They can be defined by one function of two variables, the generating function S; one possibility is $S(x', y')$ where $(x, y) \mapsto (x', y')$ according to:

$$x' = \frac{\partial S}{\partial y'}, \quad y = \frac{\partial S}{\partial x}.$$

Consider expanding S in Taylor series. The linear terms in the map are determined from the quadratic terms in S, which contain 3 group parameters, and act on 2 coordinates, f_x and f_y. The quadratic terms in the map are determined from the cubic terms in S, which contain 4 group parameters, and act on 3 coordinates, f_{xx}, f_{xy}, and f_{yy}. At order n we have $n + 2$ new group parameters acting on $n + 1$ coordinates. Thus, barring some exceptional behaviour in the action, we do not expect any invariants at generic points. This can be confirmed by considering a small image patch with $f(x, y) = x$. Let $v = \psi_y \partial/\partial_x - \psi_x \partial/\partial_y$ be the generator of an area-preserving map. The image f transforms to $x + \varepsilon\psi_y(x, y)$ which (by choosing ψ appropriately) can be any function close to x. At nongeneric points, there can be invariants. For example, the area enclosed in any level set of f is invariant. At minima or maxima of f, this will lead to invariants expressed in terms of the derivatives of f.

In the full diffeomorphism group Diff there are no differential invariants using 1 or even 2 colours (colour will be discussed in the Section 5). For example, with $k = 2$, for generic f^1, f^2 we can choose a diffeomorphism (i.e., choose local coordinates) so that $f^1 = x$ and $f^2 = y$.

5. Discussion

The recognition of objects within images as their appearance changes based on camera motion remains an unsolved problem. In this paper we have used three different methods of computing differential invariant signatures to identify appropriate signatures for images transformed under the planar Lie groups that are of interest for this question. The resulting three-dimensional signatures are not always complete, but they are relatively fast to compute. However, there are some issues that arise with turning this into a practical method.

The first is a standard issue for images: producing a computationally robust method of numerically approximating derivatives and hence invariants is not trivial, particularly for the higher-orders, where noise and rounding errors can dominate. There are three primary considerations: noise and texture; flat areas, where the derivatives are all identically zero; and the fact that conventional numerical differentiation is not well-posed [16]. Some considerations of these points and some potential approaches to solving them for practical implementations are considered by [6] and [16], but the question of how to create a full and effective method of computing numerical derivatives for images remains open. Practical approaches to using the signatures identified in this paper for real-world images will be considered in future work.

The second problem is that there are hidden symmetries within the lattice of groups we consider. For example, the relation $SA(2) \subset \mathrm{Diff}_{\mathrm{vol}}$ acts an obstruction to $SA(2)$, since many of the invariants of $SA(2)$ are also invariant under the larger

group. While there will be more invariants for the smaller group, care needs to be taken to check that the set chosen are unique to that group. The same issue arises with $A(2)$, even though $A(2)$ is not even a subgroup of $\mathrm{Diff}_{\mathrm{vol}}$.

It might be hoped that colour information can help. The formulation we provided in the introduction considered k channels of information, but so far we have considered only greyscale images ($k = 1$). Most real images are three-channel colour (RBG), and multi-spectral images can have hundreds of channels of measurement. It is therefore natural to consider whether this information is useful for the computation of invariants, in particular by allowing lower-order derivatives to form a suitable signatures. However, in practice the situation is more complicated that it first appears because the information in the channels is not independent: colour is built by the intensities in the three channels, and so there is correlation between them.

For $E(2)$, for $k \geq 2$, first derivatives suffice, but for both $SA(2)$ and $A(2)$ the hidden symmetry noted above mean that there are no signatures with only first derivatives.

The picture is more positive for the infinite-dimensional groups. For $\mathrm{Diff}_{\mathrm{con}}$, first-order signature sets are possible for $k \geq 2$ colours. They are formed from the relative invariants $(f^j_x + if^j_y)(f^m_x - if^m_y)$ of weight 2 (where f^j is the $j$the colour channel). We illustrate this using the Hopf fibration for $k = 2$. The weight 2 relative invariant

$$J = (2(f^1_x + if^1_y)(f^2_x - if^2_y), ||\nabla f^1||^2 - \|\nabla f^2\|^2)$$

obeys $\|J\|^2 = \|\nabla f^1\|^2 + \|\nabla f^2\|^2$, hence projecting to the unit sphere shows that $(f^1, f^2, J/\|J\|)$ provides a 4-dimensional signature set that is singular only when $\nabla f^1 = \nabla f^2 = 0$, a codimension 2 phenomenon for images. For $\mathrm{Diff}_{\mathrm{vol}}$ extra channels mean that different invariants now exist: there are $k(k-1)/2$ first-order invariants $\nabla f^i \times \nabla f^j$. Then the three-dimensional signature $(f^1, f^2, \nabla f^1 \times \nabla f^2)$ determines (generically and locally) the image up to an area-preserving map. We can choose the area-preserving map so that $f^1 = x$. The remaining freedom is of the area-preserving maps that preserve x: these are the shears $y \mapsto y + g(x)$. The signature for each fixed x now gives (f^2, f^2_y). This is the standard signature curve for the group of translations in y. Thus, f^2 is determined by the signature up to a translation in y, i.e., an area-preserving map.

In the full diffeomorphism group Diff there are no differential invariants using 1 or 2 colours. For example, with $k = 2$, for generic f^1, f^2 we can choose a diffeomorphism (i.e., choose local coordinates) so that $f^1 = x$ and $f^2 = y$. We therefore take $k \geq 3$. This provides the first-order relative invariants of weight 1 $\nabla f^i \times \nabla f^j$, and hence a first-order signature. However, a zeroth-order signature set is possible: $(f^1, \ldots, f^k)$, the image of the image. It is (locally and generically) complete. We can choose coordinates so that $f^1 = x$ and $f^2 = y$; then the signature locally determines $f^3, \ldots, f^k$ as functions of f^1 and f^2, i.e., the image.

Putting all of this information together, Table 3 summarises one of the most important parameters of differential invariant signatures for the transformation groups that we have considered, namely the highest order of derivative of the image that is needed. None of the groups need more than third-order differentiation, and usually less, especially for colour images.

$\mathcal{G}$	Degree $k=1$	$k=2$	$k=3$
$SE(2)$	2	1	1
$E(2)$	2	1	1
$Sim(2)$	2	1	1
$SA(2)$	2	2	2
$A(2)$	3	2	2
$PSL(2,\mathbb{C})$	3	3	3
$PSL(3,\mathbb{R})$	3	2	2
Diff_{vol}	–	1	1
Diff_{con}	3	1	1
Diff	–	–	0

Table 3: Degree (order of highest derivative of f) needed to construct a differential invariant signature of f as a function of the group $\mathcal{G}$ and the number of colours k of f. The entry '–' indicates that there is no differential invariant signature in that case.

In future work we will seek the underlying mathematical structure that we have not fully exposed. For example, all of the second-order differential invariants of $E(2)$ play known roles in geometric analysis:

- $f_x^2 + f_y^2 = \|\nabla f\|^2$ is the Lagrangian density for the Laplacian;
- $f_{xx} + f_{yy}$ is the Laplacian, which plays a key role in Euclidean and conformal geometry;
- $f_{xx}f_x^2 + 2f_{xy}f_xf_y + f_{yy}f_y^2$ is the 'infinity-Laplacian';
- $f_{xx}f_x^2 + 2f_{xy}f_xf_y + f_{yy}f_y^2$ is also a Lagrangian density for $-2(f_{xx}f_{yy} - f_{xy}^2)$, which arises in the Monge–Ampère equations and can be written in terms of the final second-order invariant as $-2(f_{xx}f_{yy} - f_{xy}^2) = 2f_{xy}^2 - f_{xx}^2 - f_{yy}^2$

Functions of these invariants are invariants or relative invariants for many groups that contain $E(2)$, such as those that we have considered in this paper. We will consider this further in future work.

Function D from Eq. (12), which appeared in $SE(2)$, $SA(2)$ and $PSL(3,\mathbb{R})$, is also known as the Bateman equation [1], and is linked to the Hodograph transformation [50].

References

[1] K. Andriopoulos, S. Dimas, P. G. L. Leach, D. Tsoubelis: *On the systematic approach to the classification of differential equations by group theoretical methods*, J. Comp. Appl. Math. 230 (2009) 224–232.

[2] R. Arora, Y. H. Hu, C. Dyer: *Estimating correspondence between multiple cameras using joint invariants*, in: Proceedings of the IEEE International Conference on Acoustics, Speech and Signal Processing, IEEE, Philadelphia (2009) 805–808.

[3] H. Bay, A. Ess, T. Tuytelaars, L. Van Gool: *SURF: Speeded up robust features*, Comp. Vision Image Understanding 110 (2008) 346–359.

[4] J. Benn, S. Marsland, R. McLachlan, K. Modin, O. Verdier: *Currents and finite elements as tools for shape space*, J. Math. Imaging Vision 61 (2019) 1197–1220.

[5] C. L. Bouton: *Some examples of differential invariants*, Bull. Amer. Math. Soc. 4 (1898) 313–322.

[6] E. Calabi, P. J. Olver, C. Shakiban, A. Tannenbaum, S. Haker: *Differential and numerically invariant signature curves applied to object recognition*, Int. J. Computer Vision 26 (1998) 107–135.

[7] E. Cartan: *La Méthode du Repère Mobile, la Théorie des Groupes Continus, et les Espaces Généralisés*, Exposés de Géometrie Vol. 5, Hermann, Paris (1935).

[8] E. Cartan: *Les problèmes d'equivalence*, Oeuvres Completes Vol. 2, Gauthiers-Villars, Paris (1952) 1311–1334.

[9] A. Cayley: *An introductory memoir on quantics*, Phil. Trans. Royal Soc. London 144 (1845) 244–258.

[10] A. Cayley: *On linear transformations*, Cambridge Dublin Math. J. 1 (1846) 104–122.

[11] O. Faugeras: *Cartan's moving frame method and its application to the geometry and evolution of curves in the Euclidean, affine and orojective planes*, in: *Applications of Invariance in Computer Vision*, J. L. Mundy, A. Zisserman, D. Forsyth (eds.), Lecture Notes in Computer Science 825, Springer, Berlin (1994) 9–46.

[12] M. Fels, P. J. Olver: *On relative invariants*, Math. Annalen 308 (1997) 701–732.

[13] M. Fels, P. J. Olver: *Moving coframes. I: A practical algorithm*, Acta Appl. Math. 51 (1998) 161–213.

[14] M. Fels, P. J. Olver: *Moving coframes. II: Regularization and theoretical foundations*, Acta Appl. Math. 55 (1999) 127–208.

[15] S. Feng, I. A. Kogan, H. Krim: *Classification of curves in 2D and 3D via affine integral signatures*, Acta Appl. Math. 109 (2010) 903–937.

[16] L. M. J. Florack, B. M. Ter Haar Romeny, J. J. Koenderink, M. A. Viergever: *Cartesian differential invariants in scale-space*, J. Math. Imaging Vision 3 (1993) 327–348.

[17] J. Flusser, J. Kautsky, F. Šroubek: *Implicit moment invariants*, Int. J. Computer Vision 86 (2009) 72–86.

[18] J.-P. Gauthier, F. Smach, C. Lemaître, J. Miteran: *Finding invariants of group actions on function spaces, a general methodology from non-Abelian harmonic analysis*, in: *Mathematical Control Theory and Finance*, A. Sarychev et al. (eds.), Proceedings of the Workshop, Lisbon 2007, Springer, Berlin (2008) 161–186.

[19] F. Ghorbel: *A complete invariant description for gray-level images by the harmonic analysis approach*, Pattern Recog. Letters 15 (1994) 1043–1051.

[20] A. González-López, N. Kamran, P. J. Olver: *Lie algebras of vector fields in the real plane*, Proc. London Math. Soc. 64 (1992) 339–368.

[21] P. Gros, L. Quan: *Projective invariants for vision*, Technical Report RT 90 IMAG-15LIFIA, INRIA (1992).

[22] C. E. Hann, M. Hickman: *Projective curvature and integral invariants*, Acta Appl. Math. 74 (2002) 177–193.

[23] M. Hickman: *Geometric moments and their invariants*, J. Math. Imaging Vision 44 (2011) 223–235.

[24] D. J. Hoff, P. J. Olver: *Extensions of invariant signatures for object recognition*, J. Math. Imaging Vision 45 (2013) 176–185.

[25] M. K. Hu: *Visual pattern recognition by moment invariants*, IRE Trans. Inform. Theory IT-8 (1962) 179–187.

[26] E. Hubert: *Differential invariants of a Lie group action: syzygies on a generating set*, J. Symbolic Computation 44 (2009) 382–416.

[27] E. Hubert, P. J. Olver: *Differential invariants of conformal and projective surfaces*, SIGMA 97 (2007), art. no. 97, 15p.

[28] R. Kakarala: *The bispectrum as a source of phase-sensitive invariants for Fourier descriptors: a group-theoretic approach*, J. Math. Imaging Vision 44 (2012) 341–353.

[29] I. A. Kogan, P. J. Olver: *Invariants of objects and their images under surjective maps*, Lobachevskii J. Math. 36 (2015) 260–285.

[30] H. Kraft, C. Procesi: *Classical Invariant Theory. A Primer*, Basel (1996).

[31] B. Kruglikov, V. Lychagin: *Global Lie-Tresse theorem*, Selecta Math. 22 (2016) 1357–1411.

[32] R. Lenz: *Group Theoretical Methods in Image Processing*, Springer, Berlin (1990).

[33] E. Li, H. Mo, D. Xu, H. Li: *Image projective invariants*, IEEE Trans. Pattern Analysis Mach. Intell. 41 (2019) 1144–1157.

[34] S. Lie: *Über Differentialinvarianten*, Math. Annalen 24 (1884) 537–578.

[35] D. E. Littlewood: *Invariant theory, tensors and group characters*, Phil. Trans. Royal Soc. London, Ser. A 239 (1944) 305–356.

[36] S. Manay, D. Cremers, B.-W. Hong, A. Yezzi, S. Soatto: *Integral invariants for shape matching*, IEEE Trans. Pattern Analysis Mach. Intell. 28 (2006) 1602–1618.

[37] E. L. Mansfield: *A Practical Guide to the Invariant Calculus*, Cambridge University Press, Cambridge (2010).

[38] S. Marsland, R. McLachlan: *Möbius invariants of shapes and images*, SIGMA 12 (2016), art. no. 80, 29p.

[39] J. L. Mundy, A. Zisserman: *Geometric Invariance in Computer Vision*, MIT Press, Cambridge, (1992).

[40] R. M. P. Negrinho, P. M. Q. Aguiar: *Shape representation via elementary symmetric polynomials: a complete invariant inspired by the bispectrum*, in: Proc. of the IEEE Int. Conf. on Image Processing, Melbourne (2013) 3518–3522.

[41] P. J. Olver: *Equivalence, Invariants and Symmetry*, Cambridge University Press, Cambridge (1995).

[42] P. J. Olver: *Classical Invariant Theory*, Cambridge University Press, Cambridge (1999).

[43] P. J. Olver: *Joint invariant signatures*, Found. Comp. Math. 1 (2001) 3–68.

[44] P. J. Olver: *A survey of moving frames*, in: *Computer Algebra and Geometric Algebra with Applications*, Proc. 6th Int. Workshop, IWMM Shanghai 2004, H. Li et al. (eds.), Lecture Notes in Computer Science 3519, Springer, Berlin (2005) 105–138.

[45] P. J. Olver: *Generating differential invariants*, J. Math. Analysis Appl. 333 (2007) 450–471.

[46] P. J. Olver: *Projective invariants of images*, https://www-users.cse.umn.edu/∼olver/mf_/prinv.pdf (2020).

[47] G. A. Papakostas, D. E. Koulouriotis, E. G. Karakasis, V. D. Tourassis: *Moment-based local binary patterns: A novel descriptor for invariant pattern recognition applications*, Neurocomputing 99 (2013) 358–371.

[48] B. C. Patterson: *The differential invariants of inversive geometry*, Amer. J. Math. 50 (1928) 553–568.

[49] B. S. Reddy, B. N. Chatterji: *An FFT-based technique for translation, rotation, and scale-invariant image registration*, IEEE Trans. Image Processing 5 (1996) 1266–1271.

[50] V. Rosenhaus: *Groups of invariance and solutions of equations determined by them*, Algebras Groups Geom. 5 (1988) 137–150.

[51] F. Smach, C. Lemaître, J.-P. Gauthier, J. Miteran, M. Atri: *Generalized Fourier descriptors with applications to objects recognition in an SVM context*, J. Math. Imaging Vision 30 (2007) 43–71.

[52] T. Suk, J. Flusser: *Point-based projective invariants*, Pattern Recognition 33 (2000) 251–261.

[53] T. Suk, J. Flusser: *Projective moment invariants*, IEEE Trans. Pattern Analysis Mach. Intell. 26 (2004) 1364–1367.

[54] A. Tresse: *Sur les invariants différentiels des groupes continus de transformations*, Acta Math. 10 (1984) 1–88.

[55] J. Turski: *Geometric Fourier analysis of the conformal camera for active vision*, SIAM Review 46 (2004) 230–255.

[56] J. Turski: *Computational harmonic analysis for human and robotic vision systems*, Neurocomputing 69 (2006) 1277–1280.

[57] L. Van Gool, T. Moons, E. Pauwels, A. Oosterlinck: *Semi-differential invariants*, in: Proceedings of a Workshop on Applications of Invariance in Computer Vision, Reykjavik 1991, J. L. Mundy and A. Zisserman (eds.), MIT Press, Cambridge (1992) 157–192.

[58] L. Van Gool, T. Moons, E. Pauwels, A. Oosterlinck: *Vision and Lie's approach to invariance*, Image Vision Comp. 13 (1995) 259–277.

[59] O. Veblen: *Differential invariants and geometry*, in: Proc. of the Int. Congress on Mathematics at Bologna 1 (1929) 181–189.

[60] J. Wood: *Invariant pattern recognition: A review*, Pattern Recognition 29 (1996) 1–17.

[61] L. Younes: *Shapes and Diffeomorphisms*, Springer, New York (2010).

[62] S. Zhang, Y. Wu, J. Chang: *Survey of image recognition algorithms*, in: Proc. of the 4th Information Technology, Networking, Electronic and Automation Control Conference (ITNEC), IEEE, Philadelphia (2020) 542–548.

[63] X. Zhang, L. R. Williams: *Euclidean invariant recognition of 2D shapes using histograms of magnitudes of local Fourier-Mellin descriptors*, in: Proceedings of the IEEE Winter Conference on Applications of Computer Vision, Hawaii 2019, IEEE, Philadelphia (2019) 303–311.

Richard Brown, Robert McLachlan, School of Information and Mathematical Sciences, Massey University, Palmerston North, New Zealand; r.g.brown@massey.ac.nz, r.mclachlan@massey.ac.nz.

Stephen Marsland, School of Mathematics and Statistics, Victoria University of Wellington, Wellington, New Zealand; stephen.marsland@vuw.ac.nz.

Received January 19, 2022
and in final form March 25, 2022